MONITORING AUTOCORRELATED PROCESSES

MONITORING AUTOCORRELATED PROCESSES

By

Weiping Tang, M.Sc.

A Thesis

Submitted to the School of Graduate Studies

in Partial Fulfilment of the Requirements

for the Degree

Master of Science

McMaster University

MASTER OF SCIENCE (2011)	McMaster University
(Statistics)	Hamilton, Ontario

TITLE:	MONITORING AUTOCORRELATED PROCESSES
AUTHOR:	Weiping Tang M.Eng. (Wuhan University of Hydraulic & Electrical Engineering, China)
SUPERVISOR:	Dr. Román Viveros-Aguilera
NUMBER OF PAGES:	xi, 88

Acknowledgements

Foremost, I would like to express my utmost gratitude to my supervisor, Dr. Román Viveros-Aguilera, for continuous support for my study and research, for his patience, motivation, enthusiasm, and immense knowledge. His guidance helped me in all the time of research and writing of this thesis. I could not have imagined having a better supervisor and mentor for my study and will never forget his sincerity.

Besides my supervisor, I would like to thank the rest of my thesis committee: Dr. Angelo Canty and Dr. Shui Feng, for their encouragement, insightful comments and challenging questions.

My sincere thanks also go to Dr. Peter Macdonald and Dr. Narayanaswamy Balakrishnan, for their encouragement and academic helps in my study.

This thesis is in memory of my father Ze Tang, and to my mother Lingxiu Hu. I would like to thank my family: my wife Zhibing Jiang, my son Ruikai Tang and my daughter Ruijun Tang, for love and support in my life.

Abstract

Several control schemes for monitoring process mean shifts, including cumulative sum (CUSUM), weighted cumulative sum (WCUSUM), adaptive cumulative sum (ACUSUM) and exponentially weighted moving average (EWMA) control schemes, display high performance in detecting constant process mean shifts. However, a variety of dynamic mean shifts frequently occur and few control schemes can efficiently work in these situations due to the limited window for catching shifts, particularly when the mean decreases rapidly. This is precisely the case when one uses the residuals from autocorrelated data to monitor the process mean, a feature often referred to as forecast recovery. This thesis focuses on detecting a shift in the mean of a time series when a forecast recovery dynamic pattern in the mean of the residuals is observed. Specifically, we examine in detail several particular cases of the Autoregressive Integrated Moving Average (ARIMA) time series models. We introduce a new upper-sided control chart based on the Exponentially Weighted Moving Average (EWMA) scheme combined with the Fast Initial Response (FIR) feature. To assess chart performance we use the well-established Average Run Length (ARL) criterion. A non-homogeneous Markov chain method is developed for ARL calculation for the proposed chart. We show numerically that the proposed procedure performs as well or better than the Weighted Cumulative Sum (WCUSUM) chart introduced by Shu, Jiang and Tsui (2008), and better than the conventional CUSUM, the ACUSUM and the Generalized Likelihood Ratio Test (GLRT) charts. The methods are illustrated on molecular weight data from a polymer manufacturing process.

Key Words: Autocorrelated data; Autoregressive integrated moving average; Average run length; Fast initial response; Adaptive CUSUM; Zero-state; Steady-state; Dynamic mean shift; Fault signature; Forecast recovery; Monte Carlo simulation; non-homogeneous Markov chain; One-sided EWMA; Smoothing parameter; Transition probability matrix; Weighted CUSUM

Contents

List of Tables

List of Figures

Chapter 1

Fault Signatures from Autocorrelated Processes

1.1 Process Monitoring

One of the most important reasons for monitoring processes, whether manufacturing or service processes, is that all of them are subject to variability. In general, there are two kinds of variability: **common cause variability** and **special cause variability** (Hawkins and Olwell 1998). Common cause variability usually comes from a process itself, such as the machine wear off, while special cause variability always comes from outside environment factors such as input material change. The statistics process control (SPC) methodologies focus on detecting special cause variability because reducing common cause always requires more fundamental process changes.

Usually, special cause variability has two categories: **transient special cause** and **persistent special cause**. Transient special cause affects a process or a system for a short while without an apparent pattern. For instance, a thunderstorm affects electrical power for a while. This kind of variability is unpredictable and rarely happens. Thus, it is very difficult to remove. Persistent special causes affect processes or systems in a persistent way and follow a pattern. For instance, it may be due to new operators or new methods involved in a process. This kind of variability happens more frequently and greatly affects process quality. SPC methodologies focus on detecting this variability and achieve tangible successes in continuous quality improvement.

Many different situations present persistent special cause variability. In general, a fixed persistent drift in the process mean is a simple situation and most of SPC methodologies can efficiently detect this kind of variability. The more complicated situation is a dynamic pattern of drift, in which the drift of a process varies over time. The objective of this thesis is to study some SPC methodologies for dynamic patterns of drift.

1.2 Autocorrelated Processes and the Forecast Recovery Phenomenon

Autocorrelated processes present typically dynamic patterns of drift. One of the popular methods for monitoring autocorrelated data is the residual chart or the special cause chart (SCC) (Alwan and Roberts 1988). It works in two steps. At first, a time-series model is fitted to remove the autocorrelation. Then a conventional control chart is applied to the model residuals. Although by this process independent residuals are obtained, however, the mean of the residuals may change over time when a step shift occurs in the mean of the original series (Shu, Jiang and Tsui, 2008). This phenomenon is referred to in the literature as **forecast recovery**.

In some time series, the forecast recovery phenomenon always occurs. When the step mean shift of data stream happens, the mean shift of its residuals typically tends to reduce over time or disappear shortly. In other words, the effect of a mean shift on the monitoring data stream is short-lived, which suggests a limited window of opportunity for catching the drift. A variety of specific situations will be discussed in the next two sections. The approach followed will be based on deriving the mean of the residuals for different time series models for the original data.

1.3 Autoregressive Integrated Moving Average Models

Autoregressive integrated moving average (ARIMA) models typically exhibit forecast recovery. An ARIMA model with p AR components, q MA components and d differences $ARIMA(p,d,q)$ for a time series $x_1, x_2, ...$ is defined as

$$x_t - \mu_0 = \frac{\theta(B)}{(1-B)^d \Phi(B)} a_t \qquad (1.1)$$

where B is the back-shift operator, $Bx_t = x_{t-1}$, $\phi(B)$ and $\theta(B)$ are polynomials of degrees p and q, respectively, and the $a_t's$ are independent and identically distributed (IID) white noise with variance σ_a^2. Here μ_0 represents the mean of the process when it is operating on target. Without loss of generality, we will take $\sigma_a^2 = 1$. Following the standard SPC approach, all the parameters are estimated from a historical (hopefully large) database, usually called Phase I data, gathered when the process was operating on-target. This can be done employing standard time series methodology (Chatifield

2004, Shumway and Stoffer 2006). This thesis will not discuss how to estimate the ARIMA model parameters, and assumes that all the on-target parameters (e.g. μ_0, σ_a^2, time series coefficients) are known. When the process is invertible, the residuals can be written as

$$y_t = \frac{(1-B)^d \phi(B)}{\theta(B)}(x_t - \mu_0) \tag{1.2}$$

If the process is in-control, the mean of the process is μ_0 indicating that no drift occurs, i.e, $\mu_0 = E(x_t)$, $t = 1, 2, \cdots$. Suppose the process mean shifts from μ_0 to $\mu_0 + \mu$ at time τ, where τ is unknown. Then $f_t = E(x_t) - \mu_0$ will be given by

$$f_t = \begin{cases} 0 & t = 1, 2, \cdots, \tau - 1; \\ \mu & t = \tau, \tau + 1, \cdots \end{cases}$$

where $\mu \neq 0$. In this situation, the residuals can be presented as (see appendix A)

$$y_t = a_t + \xi_t$$

where

$$\xi_t = \frac{(1-B)^d \phi(B)}{\theta(B)} f_t \tag{1.3}$$

is the mean pattern that takes place in the residuals.

The mean shift f_t of x_t causes a mean pattern ξ_t in the residual y_t. Consider the situation where the time series x_t follows $ARIMA(p, d, q)$ model with $p = 1, d = 0$ and $q = 1$. In this case, taking $\phi = \phi_1$ and $\theta = \theta_1$, ξ_t can be shown to be (see appendix A)

$$\xi_t = E(y_t) = \begin{cases} 0 & t = 1, 2, \cdots, \tau - 1; \\ \frac{1 - \phi + (\theta - \phi)\theta^{t-\tau}}{1-\theta}\mu & t = \tau, \tau + 1, \cdots \end{cases} \tag{1.4}$$

Although the shift f_t on the mean of x_t is constant, its effect on the mean of the residuals y_t is not, it has a dynamic pattern. The sequence ξ_t varies over time and depends on the shift that occurs at time τ. The **fault signature**, obtained by dividing the mean of the residual ξ_t by the shift's magnitude μ, is

$$FS_t = \frac{\xi_t}{\mu}. \tag{1.5}$$

For our particular case, the fault signature is

$$FS_t = \begin{cases} 0 & t = 1, 2, \cdots, \tau - 1; \\ \frac{1-\phi+(\theta-\phi)\theta^{t-\tau}}{1-\theta} & t = \tau, \tau + 1, \cdots \end{cases}$$

When time goes to infinity

$$FS_\infty = \lim_{t\to\infty} FS_t = \lim_{t\to\infty} \frac{1-\phi+(\theta-\phi)\theta^{t-\tau}}{1-\theta} = \frac{1-\phi}{1-\theta}.$$

The value of FS_∞ measures the magnitude of the tendency from the change in mean μ in the patterned mean of the residuals. If FS_∞ is close to 1, the tendency is small. Otherwise, the mean of the residuals will have a decreasing or increasing tendency. When $FS_t < 1$, the decreasing tendency indicates some degree of forecast recovery.

1.4 Some Typical Autoregressive Integrated Moving Average Models

For the purpose of comparing different control chart methods, six ARIMA(1,0,1) models have been selected for consideration, their (ϕ, θ) values are presented in Table 1.1. The same models are used by Shu, Jiang and Tsui (2008) to illustrate their methods. These models cover varying residual mean patterns ξ_t as seen in Figure 1.1

where the fault signatures for models 1-6 are plotted when $\tau = 1$ (i.e. the mean shift occurs from the very beginning) and when $\tau = 20$. The case $\tau = 1$ is referred to as **zero-state** while the case $\tau > 1$ is called a **steady-state**.

Table 1.1: Illustrative ARIMA Models

Model	ϕ	θ	FS_{∞}
Model 1	1.0	0.9	0
Model 2	0.9	0	0.1
Model 3	0.9	0.5	0.2
Model 4	0.5	-0.5	1/3
Model 5	0.5	0.5	1.0
Model 6	0.2	0.5	1.6

Model 1 with $\phi = 1$ and $\theta = 0.9$ yields a decreasing residual mean pattern that reduces practically to 0 after 50 time periods. This is a typical case found in autocorrelated process data. For Model 2 with $\phi = 0.9$ and $\theta = 0$, the residual mean shows a constant pattern after the change occurs at τ, staying at 10% of the mean shift in the original data. As with Model 1, Model 3 with $\phi = 0.9$ and $\theta = 0.5$, the residual mean also shows a decreasing pattern but the fall is much faster and leaves off at 20% of the mean shift in the original data. Typical of cases where $\theta < 0$, Model 4 with $\phi = 0.5$ and $\theta = -0.5$ produces an alternating mean residual pattern which settles down to 1/3 of the mean shift in the original time series after about 10 time periods following the change. Model 5 with $\phi = 0.5$ and $\theta = 0.5$ does not exhibit any forecast recovery, the residual mean is constant and equal to the original mean shift in the time series. For Model 6 with $\phi = 0.2$ and $\theta = 0.5$, the residual mean pattern shows the opposite of forecast recovery since, rather than decreasing, the residual mean increases quickly from the original shift to 1.6 times that shift. It takes only about 10 time periods to reach its stable value.

For Models 5 and 6, most control chart methods will work well in detecting the shift in the original time series data since the mean residual pattern stays on same or enlarged level of the original mean shift. However, it is much more challenging to detect the shift for Models 1-4 due to the magnitude of the forecast recovery and limited window to catch the mean pattern in the residuals.

Figure 1.1: ARIMA Forecast Recovery Patterns

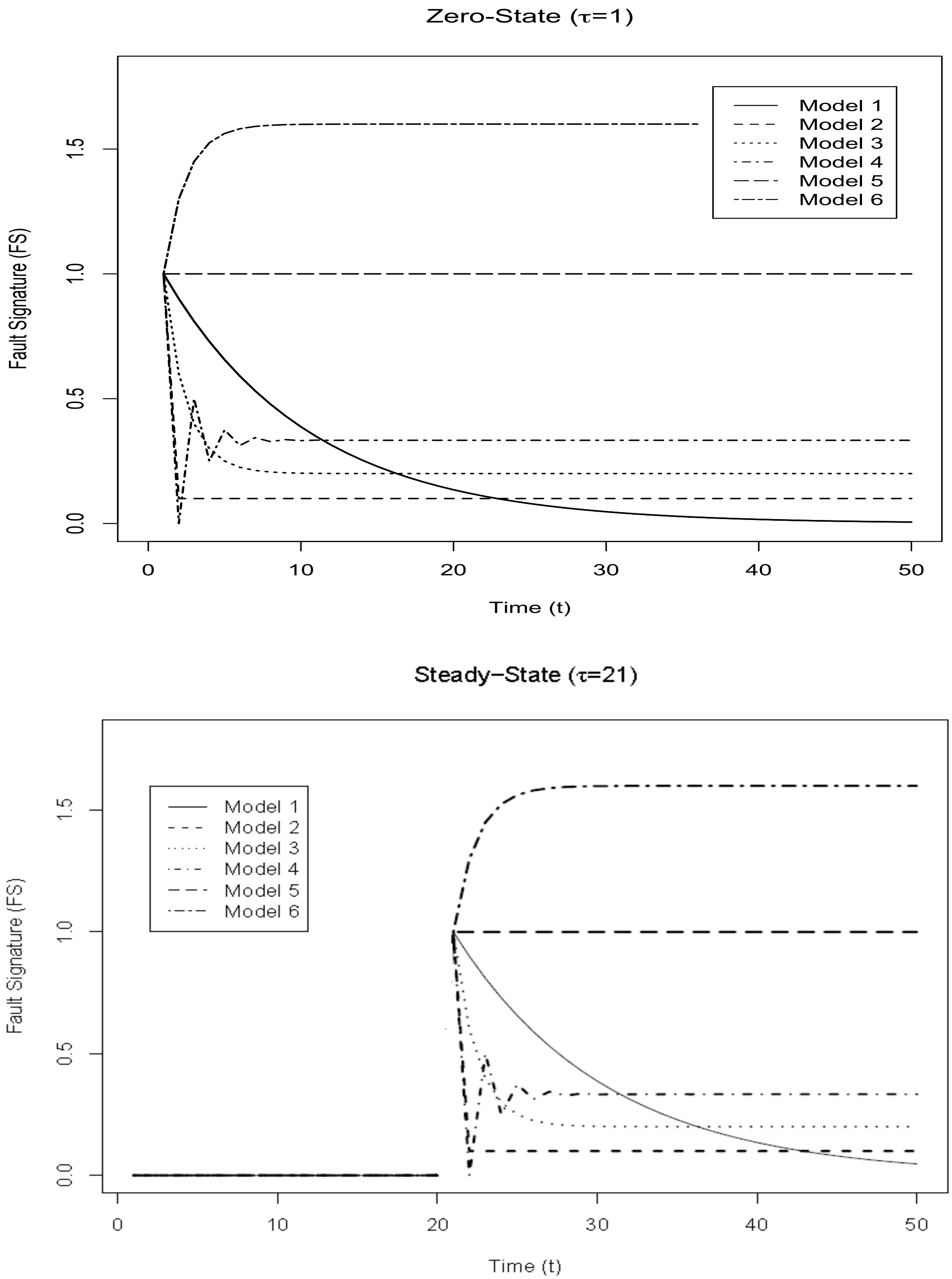

1.5 Thesis Objectives

The focus of this thesis is on control chart methods that are effective to detect mean shifts in time series data when the residuals exhibit forecast recovery. The specific objectives are:

(a) To develop in detail the upper-sided exponentially weighted moving average method for mean pattern detection in residuals from time series.

(b) To calibrate the method by developing the necessary numerics to calculate average run lengths.

(c) To compare the proposed method to the weighted CUSUM developed by Shu, Jiang and Tsui (2008).

(d) To illustrate the methods with a real data set.

The thesis is organized as follows. Chapter 1 presents a discussion of the main concepts and formulas useful to construct control charts for autocorrelated data based on residuals. These include forecast recovery, fault signature and their expression for ARIMA(1,0,1) time series models. A detailed discussion of several control chart methods for autocorrelated data is presented in Chapter 2. These include the conventional CUSUM and the weighted CUSUM. The concepts of zero-state, steady-state and fast initial response are also presented. The main contribution in the thesis is presented in Chapter 3 where the upper-sided EWMA control chart is discussed for autocorrelated process data. The analysis includes a detailed discussion of average run length calculation using a non-homogeneous Markov chain, enhancements and performance analysis. Chapter 4 compares the performance between the proposed upper-sided EWMA with FIR feature control scheme and WCUSUM control scheme, including zero-state and steady-state situations. In addition, an improved Monte Carlo simulation approach for the WCUSUM control scheme is another contribution in this thesis. An illustrative example using industrial data from Montgomery (2005) on polymer molecular weights is presented in Chapter 5. The main conclusions and recommendations of the work are presented in Chapter 6. Appendices with several derivational details are included.

Chapter 2

Control Charts for Monitoring Autocorrelated Data

Two challenging problems often encountered in quality control are the detection of changes in the mean when: a) a small persistent shift, which is less than half standard deviation, occurs, and b) when a "forecast recovery" with a dynamic mean shift pattern takes place. The second pattern in the mean is particularly difficult to detect. The main difficulty here stems from the fact that the standard methods do not react very quickly to this type of mean change, in fact, in many cases they do not react at all. However, the challenges for the two situations are different, and strategies should be different too. The difficulty with a persistent small mean shift is that the random variability is larger than the mean shift and the mean shift will be hidden in random variability. In essence, the old engineering problem of detecting a weak signal buried in noise. As for forecast recovery, the problem is the "limited window" for catching mean shift. If the opportunity is missed, it will be impossible to detect the mean shift later on. Several methodologies can be applied to detect mean shifts. Each methodology has its pros and cons for any particular case.

2.1 Cumulative Sum (CUSUM)

Walter Shewhart's Xbar and range (R) charts have been widely used for monitoring processes since 1931. However, the Xbar and R charts are not effective in detecting small to moderate shifts even if these shifts persist, mainly because these charts have no memory. The **cumulative sum** (CUSUM) chart was proposed to detect persistent process mean shifts. The main idea of the CUSUM is to use the cumulative sum of the sequence of residuals. If the CUSUM statistic falls within the decision interval, the process is considered in-control. If not, one takes the view that a process mean shift has occurred. The number of observations from the starting point up to the point at which the decision interval is crossed is called the **run length**. The run length is a random variable and its mean is called the **average run length** (ARL). For a comprehensive discussion about these and many other issues, see Montgomery (2005).

The upper-sided CUSUM statistic, denoted by W_t^U, is defined as

$$W_t^U = \max\{0, W_{t-1}^U + (y_t - k)\} \tag{2.1}$$

where y_t is the residual value at sampling period t and k is the **reference value** of the chart. When $W_t^U > h$, it signals an upward out-of-control where h is the selected upper control limit for the chart. The lower-sided CUSUM statistic, denoted by W_t^L, is similarly defined as

$$W_t^L = \min\{0, W_{t-1}^L + (z_t + k)\} \tag{2.2}$$

where z_t is the residual value at sampling period t. When $W_t^L < -h$, it signals a downward out-of-control. Assuming $y_t = -z_t$, it will be easy to see

$$W_t^U = -W_t^L \tag{2.3}$$

ARL_0 represents the average run length when the process is in control, i.e., no mean shift occurs for the process. Usually, the CUSUM is designed by picking first an acceptably large ARL_0 and then determining h and k values that achieve such ARL_0. In this thesis we work with $ARL_0 = 400$. The run length distribution of the CUSUM can be calculated by the Markov chain approach as shown in Appendix B. The CUSUM method treats the whole sequence in the same way, so it does not make any adjustment for detecting dynamic patterns in the residual mean shifts (Hu 1996).

2.2 Weighted CUSUM

Shu, Jiang and Tsui (2008) introduced their weighted CUSUM (WCUSUM) chart. Through numerical ARL calculations, they show that the WCUSUM is better than the traditional CUSUM, the Adaptive CUSUM (ACUSUM) and the Generalized Likelihood Ratio Test (GLRT) in detecting forecast recovery patterned residual mean shifts. When forecast recovery occurs, the residual y_t mean shifts quickly reduce to a low level or diminish. It is thus natural to think that putting more weight on early deviations $y_t - k$ after a shift occurs will enhance the ability to detect detecting dynamic mean shifts. The main idea of Shu's WCUSUM is to use a data-driven estimator of the feared signal to update the weights. The upper-sided WCUSUM statistic is defined as

$$W_t = \max\{0, W_{t-1} + (y_t - k)|Q_t|\} \tag{2.4}$$

where

$$Q_t = (1 - \lambda)Q_{t-1} + \lambda y_t \tag{2.5}$$

and $0 < \lambda < 1$. Note that the statistic Q_t is an exponentially weighted moving average (EWMA) scheme, which is simple and efficient (Hunter, 1986). Q_t plays a very important role in detecting patterned mean shifts because its values vary according to the sequence of residuals, thus it displays some adaptability to the evolving pattern. Shu, Jiang and Tsui (2008) use $\lambda = 0.2$.

2.3 Adaptive CUSUM

When designing the traditional CUSUM chart, the optimal reference value k is set at the half size of process mean shift magnitude, i.e., the performance of CUSUM charts is most efficient when the process mean shift magnitude is $2k$ (Moustakides 1986). Due to varying mean shift or unknown mean shift for the process, it is difficult to choose an optimal reference value k. The adaptive CUSUM overcomes this defect by using an adaptive way to change k. The core idea of ACUSUM is to adjust the reference value k in an adaptive way based on the estimation of the current process mean level (Shu, Jiang and Wu, 2008; Shu, Jiang and Tsui, 2008).

To maintain a pre-defined in-control ARL for the upper-sided CUSUM chart, the threshold h, or the decision interval, varies with the reference value k. Shu and

Jiang (2006) established the relationship between the threshold and the reference value as

$$h(k) \approx \frac{\ln[1 + 2k^2 ARL_0^U + 2.332k]}{2k} - 1.166$$

The mean shift is unknown and its estimate Q_t (Li and Wang 2010) can be used for the reference value. Note that the estimate Q_t can be close to zero when the process mean shift is estimated. Usually, the model focuses on detecting mean shifts larger than δ^+_{min}, so $\delta^+_{min}/2$ can be used as the reference value whenever $Q_t < \delta^+_{min}$.

Thus, ACUSUM is defined as

$$W_t^U = \max\left\{0, W_{t-1}^U + \frac{y_t - \hat{\delta}_t^+/2}{h(\hat{\delta}_t^+/2)}\right\} \tag{2.6}$$

where

$$\hat{\delta}_t^+ = \max\{\delta^+_{min}, Q_t\}.$$

2.4 Zero-State, Steady-State and Fast Initial Response (FIR) Feature

There are different ARLs for some control charts, depending on when the process experiences an out of control excursion. The **zero-state** operation refers to situations where the process mean shift occurs from the beginning, i.e. $\tau = 1$. The **steady-state** operation refers to situations where the process mean shift occurs at some time later, i.e. $\tau > 1$. Correspondingly, the zero-state ARL refers to the average run length calculated when the process is in the zero-state, while the steady-state ARL is the one obtained when the process is in one of the steady-states. Typically in the ARL calculations one takes $W_0 = 0$.

The **Fast initial response** (FIR) or **head start** (HS) feature refers to situations where the initial value of the control statistic is a percentage of the upper control limit h such as 50%. The objective here is to accelerate the control statistic towards the control limit when a shift to out-of-control takes place in process operation (Knoth, 2005).

Chapter 3

The Exponentially Weighted Moving Average Schemes and Enhancements

3.1 The Two-Sided EWMA

Roberts (1959) introduced the exponentially weighted moving average (EWMA) control scheme and noted its good performance in detecting a small mean shift in a process. In view of its weighting structure, the EWMA chart has alternatively been referred to as a **geometric moving average** chart. The chart has been applied largely to independent data with fixed shifts in the mean and has been studied extensively, for instance Robinson and Ho (1978), Hunter (1986), Waldmann (1986), Crowder (1987), Lucas and Saccucci (1990), and Abbasi (2010). A useful enhancement to the EWMA control scheme is the **fast initial response** (FIR) feature, which makes the scheme more sensitive to the forecast recovery patterned mean shifts discussed in this thesis.

Lucas and Saccucci (1990) furthered the study of the standard two-sided EWMA scheme and proposed a homogeneous Markov chain approach to calculate the chart's average run length. Their extensive numerical evidence reveals that the EWMA control scheme has average run length properties that are similar to those of the cumulative sum (CUSUM) control scheme. As we will see later, the homogeneous Markov chain method of Lucas and Saccucci (1990) is a special case of the more general non-homogeneous Markov chain approach developed in this thesis for the dynamic mean case.

The chart statistic is given by

$$W_t = (1-\lambda)W_{t-1} + \lambda y_t, \quad t = 1, 2, 3, ... \tag{3.1}$$

where λ is the **smoothing parameter** $(0 < \lambda \leq 1)$, W_0 is the initial value of the statistic (typically set at 0) and y_t is the observed data at the t-th sampling period, in our case the observed residual. Usually the residuals are standardized so that when the process operates on target they have a mean of 0 and a variance of 1. As a result, if the residuals are normally distributed so will be W_t with mean 0 when the process operates on-target, thus the natural control limits are $\pm h$ where $h > 0$. The role of λ will be examined in more detail later when the numerical work is presented

Different approaches are available to design and calibrate a control chart. In this thesis we follow the method most widely used which is based on control limits and average run lengths. We do this in combination with the FIR feature to enhance performance.

3.2 The Upper-Sided EWMA

In practice, one usually looks for an upward mean shift or a downward mean shift. This leads to working with the one-sided EWMA, one chart for shifts above the target process mean (upper-sided) and one for shifts to values below the target mean (lower sided). This tuning of the method makes the chart more efficient.

Of particular interest in this thesis is the upper-sided EWMA. The relevant statistic is defined as

$$W_t^+ = \max\{0, (1-\lambda)W_{t-1}^+ + \lambda y_t\}, \quad t = 1, 2, 3, ... \tag{3.2}$$

where λ and y_t are as for the two-sided EWMA, and W_0^+ is typically set at 0. The chart is intended for detection of shifts in the process mean to values larger than the target mean. By taking the maximum in eqn. (3.2), we are effectively adopting a resetting mechanism that prevents the statistic from venturing into negative values which are of no relevance when one aims to detect increases in the mean. Clearly $W_t^+ \geq 0$ for all t and large values of the statistic are indicative of a possible upward jump in the mean. Thus we need only an upper control limit $h > 0$. When $W_t^+ > h$, an out-of-control signal is issued associated with an upward trend in the process mean.

3.3 Markov Chain Approach for Average Run Length (ARL) Calculation

As noted earlier, the **average run length** (ARL) is the key measure used in the quality control literature to assess the performance of a control chart and to compare charts. It is defined as

$$ARL = E(RL),$$

where RL is the **run length**, that is, the number of process runs until the chart jumps out of the control limit(s) for the first time across sampling periods. In other words, the ARL is the number of runs one would expect to observe on the average until the chart signals for the first time an out-of-control excursion in process operation.

Two types of ARLs are of interest. One is the **in-control** ARL, denoted by ARL_0, which is the expected number of runs until the chart signals when the process operates on-target. In other words, the average number of runs until a false alarm occurs. This is an undesirable call and thus should not happen very often. In practice, the control limits are selected in such a way that ARL_0 is large, $ARL_0 = 400$ or 500 in this thesis. The other type of ARL, denoted by ARL_1 is the average number of runs until the chart signals when indeed the process has moved to an out-of-control state. Naturally efficient charts are those for which ARL_1 values are small. ARL_1 is referred to as the **out-of-control** ARL.

As discussed earlier, the aim is to use the residuals $y_1, y_2, y_3, ...$ from a time series model to build control charts for the mean μ of the original time series measurements $x_1, x_2, x_3, ...$ as proposed and illustrated by Shu, Jiang and Tsui (2008). However, unlike the standard setting for control charts where a step change in the mean of the measurements used in the monitoring occurs, a dynamic pattern in the mean ξ_t of y_t is shown as described by the forecast recovery eqn. (1.3). Following Shu, Jiang and Tsui (2008), we will assume that the residuals $y_1, y_2, y_3, ...$ are independent and normally distributed with a common variance, $y_t \sim N(\xi_t, \sigma^2)$. When the process operates in-control, $\xi_t = 0$ for all t.

Appendix B contains a detailed presentation on run length distribution and average run length calculations. Non-homogeneous and homogeneous Markov chains are involved. We focus on the equations for average run length calculation, a summary of these equations is presented here.

Two-Sided EWMA. From Appendix B, the average run length is obtained from a non-homogeneous Markov chain as

$$ARL_1 = \sum_{n=1}^{\infty} n\boldsymbol{p}_0' \left(\prod_{l=1}^{n-1} \boldsymbol{P}_l \right) (\boldsymbol{I} - \boldsymbol{P}_n)\mathbf{1}, \tag{3.3}$$

where $\boldsymbol{P}_t$ is the $(2m+1) \times (2m+1)$ transition probability matrix from sampling period $t-1$ to t, given by

$$\begin{aligned} P_{ij}^{(t)} &= \Phi\left(\frac{1}{\sigma}\left\{\frac{L}{\lambda}[2(j-(1-\lambda)i)+1] - h - L - \xi_t\right\}\right) \\ &\quad -\Phi\left(\frac{1}{\sigma}\left\{\frac{L}{\lambda}[2(j-(1-\lambda)i)-1] - h - L - \xi_t\right\}\right), \end{aligned} \tag{3.4}$$

where m is a positive integer (see eqn. (B.3)), $L = n/(2m+1)$ and $\Phi(\cdot)$ is the standard normal distribution function. In eqn. (3.3), $\boldsymbol{p}_0$ is the $(2m+1) \times 1$ chain's initial probability vector usually taken to have 1 at entry $m+1$ and 0s at every other entry, and $\mathbf{1}$ is the $(2m+1) \times 1$ vector of 1s. Strictly speaking the above are approximations with the right-hand-side of (3.3) converging to the exact ARL as $m \to \infty$. In the numerical cases discussed here, using $m = 50$ for a total of about 100 states in the chain gives satisfactory results. When the process is on target, the mean in the original x data remains constant at $\mu = \mu_0$, as a result $\xi_t = 0$ for all t. In this case the Markov chain is homogeneous and the ARL can be worked out in closed form resulting in

$$ARL_0 = \boldsymbol{p}_0'(I - \boldsymbol{P}_0)^{-1}\mathbf{1}, \tag{3.5}$$

where $\boldsymbol{P}_0$ is the $(2m+1) \times (2m+1)$ common transition probability matrix obtained from (3.4) by taking $\xi_t = 0$.

Upper-Sided EWMA. As discussed in Appendix B, ARL equations (3.3) and (3.5) also apply to this case but with $\boldsymbol{P}_t$ replaced with the $m \times m$ transition probability matrix with entries

$$P_{ij}^{(t)} = \begin{cases} \Phi\left(\frac{1}{\sigma}\left\{\frac{L}{\lambda}[2(1-(1-\lambda)(i-1))-1]-\xi_t\right\}\right), \quad j=1; \\ \\ \Phi\left(\frac{1}{\sigma}\left\{\frac{L}{\lambda}[2(j-(1-\lambda)(i-1)-1]-\xi_t\right\}\right) \\ -\Phi\left(\frac{1}{\sigma}\left\{\frac{L}{\lambda}[2(j-(1-\lambda)(i-1)-3]-\xi_t\right\}\right), \quad j \geq 2. \end{cases} \tag{3.6}$$

Here the chain's initial probability vector $\boldsymbol{p}_0$ is the $m \times 1$ vector usually taken to have 1 in the first entry and 0s at every other entry, and $\mathbf{1}$ is the $m \times 1$ vector of 1s. In this case, $m = 100$ gives satisfactory results for all the numerical cases considered.

3.4 Numerical Performance

We focus now on the numerical ARL performance of the two-sided and the upper-sided EWMA charts in detecting dynamic changes in the mean. The particular scenarios considered are the 6 ARIMA(1,0,1) time series models detailed in Table 1.1. The ARL results are presented in Tables 3.1-3.3. The specifics of the numerical work were as follows.

- The in-control mean for the original x values was set at $\mu_0 = 0$ and the variance at $\sigma^2 = 1$.

- Upward step changes in μ from $\mu_0 = 0$ to μ_1 were considered ranging from $\mu_1 = 0.1$ to $\mu_1 = 4.0$, the change taking place at $\tau = 1$ (the zero-state situation).

- The above step changes in μ induced dynamic changes in the mean ξ_t of the y residuals, calculated from the forecast recovery eqn. (1.4) and graphed in the upper plot of Figure 1.1.

- The in-control mean was set at $ARL_0 = 400$ and was calculated using eqn. (3.5). The control limit h was obtained iteratively until ARL_0 was close enough to its set value of 400.

- The out-of-control average run length ARL_1 was calculated using eqn. (3.3). The number of terms kept in the series was 5000, this number of terms gave stable results.

- Three values of the smoothing parameter were used, namely $\lambda = 0.2$, 0.1 and 0.05, one table for each value of λ. The default value typically used is $\lambda = 0.1$.

An examination of Tables (3.1)-(3.3) reveals the following trends.

(1) Perhaps the most notable feature is the superiority of the upper-sided EWMA.

(2) For small jumps in μ, small λ produces slightly better results, i.e. smaller ARL_1 values, while the opposite occurs for large jumps in μ.

(3) Comparing Models 1 and 3, we can see that for both EWMAs, the lower the fast recovery falls, the larger the ARL_1, i.e. the longer it takes to signal the change.

(4) The best performance for both methods is shown in Model 6 where, one can see from the upper plot in Figure 1.1, the mean of the residuals exhibits an increasing pattern, somewhat the opposite of fast recovery.

Table 3.1: Zero-State ARL Comparisons Between the Upper-Sided EWMA and the Two-Sided EWMA ($\lambda = 0.2$)

Model		Model 1		Model 2		Model 3		Model 4		Model 5		Model 6	
ϕ		1		0.9		0.9		0.5		0.5		0.2	
θ		0.9		0		0.5		-0.5		0.5		0.5	
Type		One-sided	Two-sided	One-sided	Two-sided	One-sided	Two-sided	One-sided	Two-sided	One-sided	Two-sided	One-sided	Two-sided
h		0.930427	0.9644	0.930427	0.9644	0.930427	0.9644	0.930427	0.9644	0.930427	0.9644	0.930427	0.9644
μ	0	399.9981	399.8435	399.9981	399.8435	399.9981	399.8435	399.9981	399.8435	399.9981	399.8435	399.9981	399.8435
	0.1	**394.2188**	398.768	**374.4536**	398.5267	**350.5881**	394.728	**322.068**	386.3394	**212.7215**	303.4709	**149.9471**	218.6289
	0.2	**386.9327**	395.5667	**350.704**	394.7084	**307.7914**	380.1598	**260.8454**	350.619	**119.8768**	171.9926	**65.87953**	87.0789
	0.3	**377.7867**	390.0765	**328.601**	388.5238	**270.6455**	357.9723	**212.5538**	303.2057	**71.92148**	96.35277	**34.22094**	41.41324
	0.4	**366.3611**	381.9949	**308.013**	380.141	**238.3401**	330.5968	**174.2992**	254.0839	**46.00503**	57.83423	**20.71128**	23.77547
	0.5	**352.4097**	371.1323	**288.8332**	369.8918	**210.1853**	300.5356	**143.8591**	209.3367	**31.30606**	37.51936	**14.17267**	15.76177
	1	**239.727**	268.1413	**210.5637**	300.6526	**113.8846**	164.0325	**60.92744**	79.59979	**9.224577**	9.98351	**5.411293**	5.681615
	1.5	**99.4664**	120.7058	**154.5738**	226.0442	**62.12573**	84.05226	**30.41559**	36.32064	**5.036461**	5.298266	**3.570137**	3.691737
	2	**17.30417**	22.28583	**113.5214**	160.9319	**33.08922**	42.51577	**17.49545**	19.85016	**3.490132**	3.63067	**2.771038**	2.848641
	2.5	**3.97578**	4.598253	**82.98712**	115.2005	**16.85081**	20.94888	**11.19824**	12.3664	**2.712429**	2.804865	**2.317208**	2.372434
	3	**2.453088**	2.560871	**59.33347**	80.4594	**8.313846**	10.06807	**7.692241**	8.392226	**2.260535**	2.326893	**2.050167**	2.087796
	4	**1.791267**	1.853713	**26.0654**	35.00346	**2.52289**	2.818117	**3.943643**	4.319708	**1.766223**	1.822161	**1.744554**	1.793542

Table 3.2: Zero-State ARL Comparisons Between the Upper-Sided EWMA and the Two-Sided EWMA ($\lambda = 0.1$)

Model		Model 1		Model 2		Model 3		Model 4		Model 5		Model 6	
ϕ		1		0.9		0.9		0.5		0.5		0.2	
θ		0.9		0		0.5		-0.5		0.5		0.5	
Type		One-sided	Two-sided	One-sided	Two-sided	One-sided	Two-sided	One-sided	Two-sided	One-sided	Two-sided	One-sided	Two-sided
h		0.6088623	0.628	0.6088623	0.628	0.6088623	0.628	0.6088623	0.628	0.6088623	0.628	0.6088623	0.628
μ	0	400.0556	400	400.0556	400	400.0556	400	400.0556	400	400.0556	400	400.0556	400
	0.1	**393.8751**	398.3259	**368.789**	397.5223	**340.2003**	391.4825	**306.5783**	378.2779	**186.6351**	264.6123	**124.7893**	172.4985
	0.2	**385.9886**	394.4802	**340.2891**	391.455	**290.359**	368.9558	**237.6693**	325.8583	**97.32083**	129.6203	**52.04421**	63.04669
	0.3	**375.9874**	387.8945	**314.2801**	381.7545	**248.722**	336.4543	**186.468**	264.2207	**56.7929**	69.53646	**28.09371**	31.79893
	0.4	**363.4089**	378.255	**290.5218**	368.9077	**213.8241**	299.1368	**148.1023**	208.3355	**36.72457**	42.5538	**18.26232**	20.0159
	0.5	**347.9723**	365.3642	**268.8047**	353.5868	**184.4727**	261.3176	**119.0993**	163.3008	**25.87218**	28.98213	**13.38621**	14.4066
	1	**225.1902**	248.5097	**184.7149**	261.2505	**92.53061**	122.4157	**48.00083**	57.15141	**9.379365**	9.887934	**6.000246**	6.230526
	1.5	**84.44447**	99.2586	**129.5888**	179.4464	**49.3985**	59.87784	**25.01821**	27.74595	**5.66303**	5.873743	**4.113353**	4.225473
	2	**14.18245**	17.05184	**92.52162**	121.9039	**27.29968**	31.42929	**15.5646**	16.71895	**4.101196**	4.227486	**3.240194**	3.314496
	2.5	**4.281144**	4.629188	**66.96836**	84.29357	**15.32373**	17.21859	**10.8255**	11.4554	**3.251581**	3.342608	**2.725858**	2.78659
	3	**3.001543**	3.106091	**48.86515**	59.23245	**8.753176**	9.718983	**8.079715**	8.489318	**2.715753**	2.788237	**2.354605**	2.406111
	4	**2.196571**	2.245874	**25.91919**	30.1097	**3.43964**	3.70686	**5.088914**	5.32785	**2.11349**	2.150394	**2.003564**	2.017956

Table 3.3: Zero-State ARL Comparisons Between the Upper-Sided EWMA and the Two-Sided EWMA ($\lambda = 0.05$)

Model		Model 1		Model 2		Model 3		Model 4		Model 5		Model 6	
ϕ		1		0.9		0.9		0.5		0.5		0.2	
θ		0.9		0		0.5		-0.5		0.5		0.5	
Type		One-sided	Two-sided	One-sided	Two-sided	One-sided	Two-sided	One-sided	Two-sided	One-sided	Two-sided	One-sided	Two-sided
h		0.3937305	0.4050293	0.3937305	0.4050293	0.3937305	0.4050293	0.3937305	0.4050293	0.3937305	0.4050293	0.3937305	0.4050293
μ	0	399.9288	400	399.9288	400	399.9288	400	399.9288	400	399.9288	400	399.9288	400
	0.1	**393.7954**	398.9084	**363.1981**	397.1957	**330.346**	388.4187	**292.4858**	369.6499	**166.6738**	230.7947	**108.1894**	141.3385
	0.2	**385.9774**	394.9005	**330.4162**	388.3797	**274.7572**	356.8167	**218.3747**	300.9492	**83.8276**	104.7252	**46.00022**	53.00858
	0.3	**376.0724**	388.063	**301.1113**	374.5407	**230.1056**	314.1447	**166.5072**	230.2555	**49.80223**	57.70223	**26.73384**	29.40462
	0.4	**363.6287**	378.1162	**274.8775**	356.7231	**194.0348**	268.9891	**129.6447**	173.886	**33.62803**	37.43661	**18.56032**	19.97323
	0.5	**348.3569**	364.8885	**251.3612**	336.1592	**164.7222**	226.9181	**103.0238**	132.8932	**24.85871**	27.04915	**14.24554**	15.12872
	1	**226.7233**	247.1563	**164.8451**	226.6216	**79.67229**	97.65972	**42.57685**	48.03521	**10.45573**	10.90451	**6.924856**	7.153123
	1.5	**86.33647**	99.00649	**112.4883**	146.2143	**43.61337**	49.15511	**24.01777**	25.77551	**6.64279**	6.847904	**4.819495**	4.935905
	2	**15.66478**	18.14661	**79.48576**	97.07564	**25.90436**	28.11828	**16.06048**	16.88029	**4.912898**	5.043222	**3.807826**	3.887062
	2.5	**5.284412**	5.622156	**57.82297**	67.2635	**16.19567**	17.35779	**11.80882**	12.2974	**3.93344**	4.029928	**3.209715**	3.268548
	3	**3.777445**	3.896724	**43.04917**	48.40951	**10.49245**	11.21608	**9.20281**	9.545205	**3.310067**	3.386517	**2.83244**	2.884595
	4	**2.712547**	2.787952	**25.03684**	27.20826	**4.920408**	5.239491	**6.205084**	6.422924	**2.537577**	2.602322	**2.207273**	2.252519

3.5 Enhancements

3.5.1 The Effect of the Smoothing Parameter λ

To facilitate understanding the effect of λ, consider the two-sided EWMA statistic from eqn. (3.1). Expanding the right-hand-side recursively leads to

$$W_t = (1-\lambda)W_{t-1} + \lambda y_t = \lambda \sum_{i=0}^{t-1}(1-\lambda)^i y_{t-i} + (1-\lambda)^t W_0, \tag{3.7}$$

where $y_t \sim N(\xi_t, \sigma^2)$, $W_0 = 0$ and $0 < \lambda \leq 1$. Hence,

$$E(W_t) = \lambda \sum_{i=0}^{t-1}(1-\lambda)^i \xi_{t-i}, \quad Var(W_t) = \lambda^2 \left(\sum_{i=0}^{t-1}(1-\lambda)^{2i}\right)\sigma^2 = \frac{1-(1-\lambda)^{2t}}{1-(1-\lambda)^2}\lambda^2\sigma^2,$$

from which we can see that $\lim_{t\to\infty} Var(W_t) = \lambda\sigma^2/(2-\lambda)$ for $0 < \lambda \leq 1$.

Eqn. (3.7) shows clearly that W_t is a weighted average of the current and previous residuals $y_t, y_{t-1}, ..., y_1$. Moreover, the weights are determined entirely by the smoothing parameter λ. It is clear that the smaller the value of λ, the smaller the weight of the current residual thus the greater the impact of the previous residuals. In other words, small λ translates into more weight for the "history" W_{t-1}. One would expect therefore that a persistent small shift in μ will be more effectively detected using a small λ.

With this in mind, consider the performance of the upper-sided EWMA chart. Figure 3.1 contains graphs of the ARL for three values of λ, namely $\lambda = 0.2$, 0.1 and 0.05, and for each of the 6 ARIMA(1,0,1) time series models from Table 1.1. Other than Model 2, for all models the graphs show that a chart with small λ detects small mean shifts faster, while large mean shifts are more effectively detected by charts with large λ. The pattern for Model 2 shows somewhat similar performance at small and

Figure 3.1: The Effect of λ for the Upper-Sided EWMA ARL

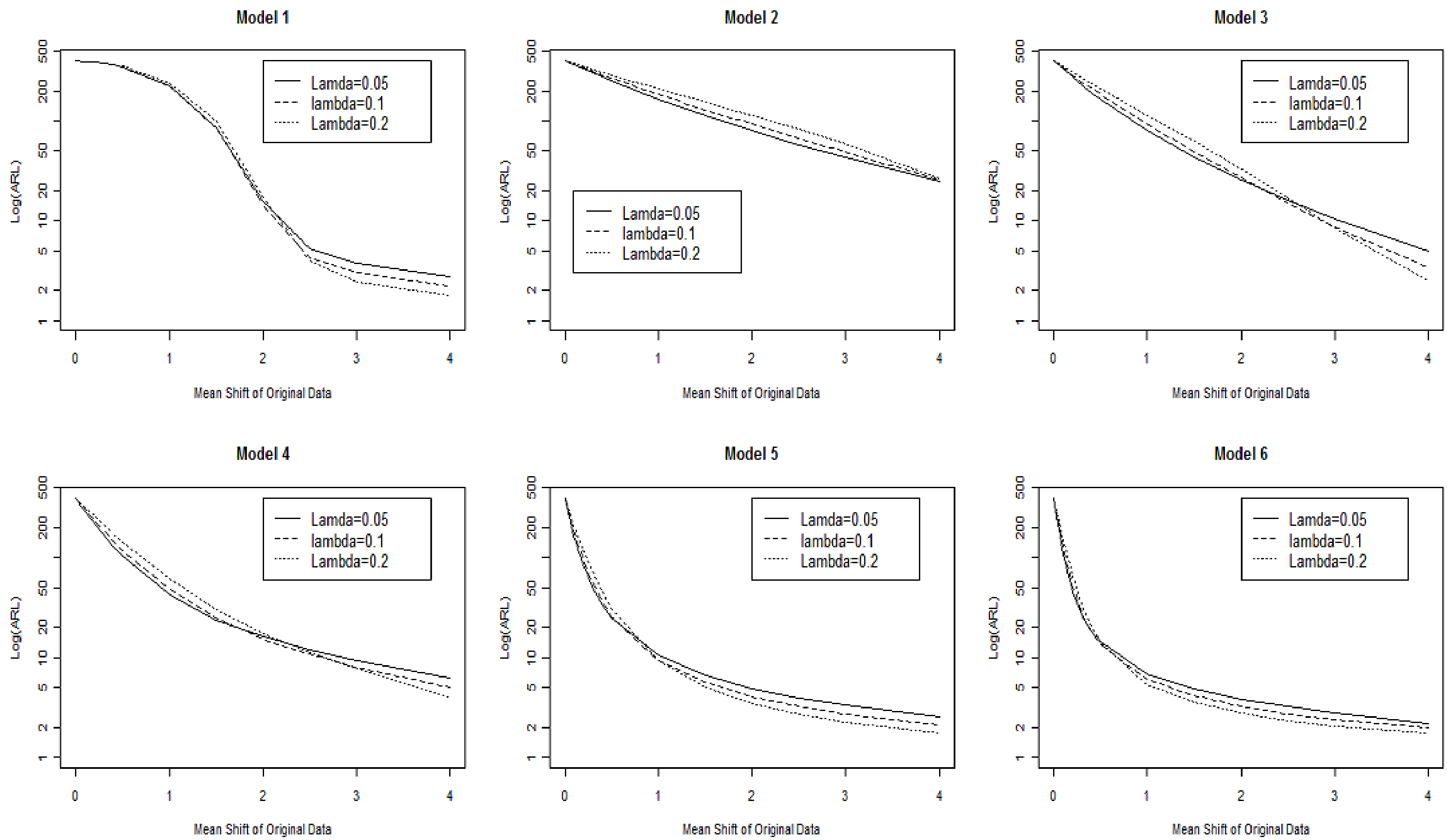

large mean shifts but a better performance for charts with small λ for mean jumps of moderate size.

3.5.2 The Effect of the Fast Initial Response

Lucas and Saccucci (1990) put forward the concept of **fast initial response** (FIR) for the two-sided EWMA in the context of step shifts in process mean. They showed numerically that substantive increases in chart efficiency can result when the mean shift occurs early on in process operation. We expect that even a more dramatic impact will be felt for the fast recovery mean patterns considered here.

The basic idea of the FIR feature is that, rather than starting the chart at $W_0 = 0$. it should start at some other value. This will give an initial boost to the chart. We will discuss the FIR feature for the upper-sided EWMA, the chart that tends to perform better compared to the two-sided EWMA. With h as the upper control limit, i.e. $[0, h]$ as the decision interval, the chart will have initial value

$$W_0^+ = ph,$$

where $0 \leq p \leq 1$. By working with the respective percentage, we say that the chart is given a head start of $100p\%$.

The method was applied to the upper-sided EWMA for the 6 ARIMA(1,0,1) models and λ values that have been discussed so far. The numerical results are tabulated in Tables 3.4-3.9. The same results are displayed graphically in Figures 3.2-3.4. Each table contains the results for 3 time series models, one value of λ and 4 head start values, namely 0% (the case of $W_0^+ = 0$ that has been considered so far), 25%, 50% and 75%. The main patterns noted from the tables and figures are as follow.

(1) For all 6 models, substantive improvements in ARL are noted, particularly for large values of the mean shift.

(2) In general, the larger the head start, the better the chart performs.

(3) Note that the control limit h is adjusted for every level of head start. In general, the greater the head start, the larger the value of h. This should have been expected since starting from a larger value W_0^+ will lead to reach quicker the control limit h on average even if no change in the process mean occurs, and thus the value of h has to be increased to keep $ARL_0 = 400$.

(4) The effect of the degree of smoothing λ is somewhat less apparent, perhaps easier to appreciate or small mean shifts: the greater the head start and the smaller the value of λ, the better the chart performance.

Table 3.4: The Upper-Sided EWMA Zero-State ARL for Model 1, 2 and 3 with Different Head Starts ($\lambda = 0.2$)

Model		Model 1				Model 2				Model 3			
ϕ		1				0.9				0.9			
θ		0.9				0				0.5			
HS		0	25%	50%	75%	0	25%	50%	75%	0	25%	50%	75%
h		0.930427	0.9312275	0.9333317	0.9403742	0.930427	0.9312275	0.9333317	0.9403742	0.930427	0.9312275	0.9333317	0.9403742
μ	0	399.9981	400	400	400	399.9981	400	400	400	399.9981	400	400	400
	0.1	394.2188	393.0503	390.027	**383.9675**	374.4536	374.1308	372.7682	**369.0456**	350.5881	349.9386	347.9165	**343.11**
	0.2	386.9327	384.0406	377.549	**364.7055**	350.704	349.9514	347.4403	**340.0086**	307.7914	306.4163	302.7415	**293.7872**
	0.3	377.7867	372.6713	362.0831	**342.0998**	328.601	327.4202	323.7537	**312.7241**	270.6455	268.5748	263.3943	**250.9916**
	0.4	366.3611	358.505	343.3013	**316.1704**	308.013	306.4032	301.5681	**287.0604**	238.3401	235.6023	229.0603	**213.8656**
	0.5	352.4097	341.343	321.2278	**287.453**	288.8332	286.7923	280.7735	**262.9347**	210.1853	206.8094	199.0506	**181.6803**
	1	239.727	212.1163	174.8303	**129.3926**	210.5637	206.2651	194.0581	**162.6172**	113.8846	107.8714	96.3219	**75.80774**
	1.5	99.4664	75.49807	51.29571	**29.90202**	154.5738	147.6816	129.2838	**91.744**	62.12573	54.87209	43.42993	**28.00715**
	2	17.30417	11.39112	6.721225	**3.479821**	113.5214	103.6219	80.61451	**45.82721**	33.08922	26.33769	17.79029	**9.253565**
	2.5	3.97578	2.936295	2.056314	**1.398912**	82.98712	70.01883	45.89966	**20.09532**	16.85081	11.84276	6.82151	**3.136022**
	3	2.453088	1.990074	1.493013	**1.146115**	59.33347	44.22652	23.25193	**7.839003**	8.313846	5.26008	2.81709	**1.488639**
	4	1.791267	1.402575	1.116116	**1.016936**	26.0654	13.15937	4.38527	**1.495663**	2.52289	1.650901	1.169571	**1.023507**

Table 3.5: The Upper-Sided EWMA Zero-State ARL for Model 4, 5 and 6 with Different Head Starts ($\lambda = 0.2$)

Model		Model 4				Model 5				Model 6			
ϕ		0.5				0.5				0.2			
θ		-0.5				0.5				0.5			
HS		0	25%	50%	75%	0	25%	50%	75%	0	25%	50%	75%
h		0.930427	0.9312275	0.9333317	0.9403742	0.930427	0.9312275	0.9333317	0.9403742	0.930427	0.9312275	0.9333317	0.9403742
μ	0	399.9981	400	400	400	399.9981	400	400	400	399.9981	400	400	400
	0.1	322.068	321.5572	319.9491	**315.9415**	212.7215	211.6988	209.2571	**204.0763**	149.9471	148.8457	146.4216	**141.5406**
	0.2	260.8454	259.8633	257.242	**250.4026**	119.8768	118.4571	115.4579	**109.3802**	65.87953	64.65636	62.28868	**57.90257**
	0.3	212.5538	211.2161	207.8696	**199.148**	71.92148	70.41086	67.47484	**61.90826**	34.22094	33.10294	31.13453	**27.79732**
	0.4	174.2992	172.6946	168.8395	**158.9388**	46.00503	44.52786	41.85611	**37.12477**	20.71128	19.72343	18.11465	**15.58754**
	0.5	143.8591	142.0561	137.8548	**127.2918**	31.30606	29.90924	27.54074	**23.6089**	14.17267	13.2979	11.96153	**9.985868**
	1	60.92744	58.72462	54.10867	**44.15928**	9.224577	8.259322	6.955896	**5.234984**	5.411293	4.851828	4.136039	**3.219155**
	1.5	30.41559	28.23017	24.01317	**16.63105**	5.036461	4.342024	3.499478	**2.509976**	3.570137	3.14661	2.636318	**2.013054**
	2	17.49545	15.41573	11.75628	**6.799724**	3.490132	2.961102	2.340548	**1.676099**	2.771038	2.42949	2.016302	**1.532465**
	2.5	11.19824	9.210178	6.159297	**3.106699**	2.712429	2.289523	1.785555	**1.315492**	2.317208	2.040281	1.667901	**1.278214**
	3	7.692241	5.785003	3.404366	**1.713781**	2.260535	1.895361	1.45897	**1.138218**	2.050167	1.795957	1.425975	**1.131147**
	4	3.943643	2.422412	1.39478	**1.056462**	1.766223	1.3957	1.11489	**1.016806**	1.744554	1.390953	1.114184	**1.01674**

Table 3.6: The Upper-Sided EWMA Zero-State ARL for Model 1, 2 and 3 with Different Head Starts ($\lambda = 0.1$)

Model		Model 1				Model 2				Model 3			
ϕ		1				0.9				0.9			
θ		0.9				0				0.5			
HS		0	25%	50%	75%	0	25%	50%	75%	0	25%	50%	75%
h		0.6088623	0.6097681	0.6125134	0.6210254	0.6088623	0.6097681	0.6125134	0.6210254	0.6088623	0.6097681	0.6125134	0.6210254
μ	0	400.0556	400	400	400	400.0556	400	400	400	400.0556	400	400	400
	0.1	393.8751	391.5711	386.7496	**375.86**	368.789	368.0157	366.4823	**360.9846**	340.2003	338.9247	336.142	**328.2626**
	0.2	385.9886	380.754	369.9493	**347.9095**	340.2891	338.9102	335.8618	**325.6774**	290.359	288.0766	282.9062	**269.2995**
	0.3	375.9874	367.0003	349.3271	**316.2445**	314.2801	312.3307	307.8807	**293.4429**	248.722	245.5526	238.426	**220.614**
	0.4	363.4089	349.8657	324.7639	**281.5155**	290.5218	288.034	282.2837	**263.9951**	213.8241	209.873	201.1637	**180.4199**
	0.5	347.9723	329.2151	296.6419	**245.0349**	268.8047	265.8089	258.8518	**237.1058**	184.4727	179.8345	169.8689	**147.2522**
	1	225.1902	183.5377	133.2392	**81.19567**	184.7149	179.5689	167.7126	**134.1254**	92.53061	85.67281	73.15736	**51.32957**
	1.5	84.44447	54.46097	29.84573	**13.10294**	129.5888	122.8205	107.5147	**70.50109**	49.3985	42.05737	31.0289	**16.77303**
	2	14.18245	8.097449	4.339958	**2.146733**	92.52162	84.53404	67.01444	**33.64763**	27.29968	20.78797	12.9168	**5.500697**
	2.5	4.281144	3.12146	2.202406	**1.38593**	66.96836	58.07049	39.76647	**14.46808**	15.32373	10.35285	5.564155	**2.218685**
	3	3.001543	2.388077	1.749637	**1.173199**	48.86515	39.31576	21.97648	**5.774722**	8.753176	5.413811	2.779155	**1.335405**
	4	2.196571	1.806993	1.265679	**1.023327**	25.91919	16.12193	5.31482	**1.358299**	3.43964	2.207228	1.330163	**1.027007**

Table 3.7: The Upper-Sided EWMA Zero-State ARL for Model 4, 5 and 6 with Different Head Starts ($\lambda = 0.1$)

Model		Model 4				Model 5				Model 6			
ϕ		0.5				0.5				0.2			
θ		-0.5				0.5				0.5			
HS		0	25%	50%	75%	0	25%	50%	75%	0	25%	50%	75%
h		0.6088623	0.6097681	0.6125134	0.6210254	0.6088623	0.6097681	0.6125134	0.6210254	0.6088623	0.6097681	0.6125134	0.6210254
μ	0	400.0556	400	400	400	400.0556	400	400	400	400.0556	400	400	400
	0.1	306.5783	305.3695	302.8489	**296.0364**	186.6351	184.5803	180.1997	**170.8131**	124.7893	122.6313	118.1775	**109.4761**
	0.2	237.6693	235.7235	231.5489	**221.0118**	97.32083	94.8226	89.84992	**80.38903**	52.04421	49.91963	45.99619	**39.40726**
	0.3	186.468	184.0263	178.8616	**166.4022**	56.7929	54.32096	49.79373	**42.01749**	28.09371	26.25423	23.19897	**18.62514**
	0.4	148.1023	145.3343	139.6262	**126.3909**	36.72457	34.41726	30.51929	**24.38669**	18.26232	16.68285	14.27932	**10.96053**
	0.5	119.0993	116.1251	110.1718	**96.87139**	25.87218	23.75801	20.43807	**15.58165**	13.38621	12.01293	10.06263	**7.510896**
	1	48.00083	44.88679	39.55414	**29.45095**	9.379365	8.013376	6.31725	**4.271**	6.000246	5.172229	4.183345	**2.997889**
	1.5	25.01821	22.2598	18.07116	**11.15535**	5.66303	4.697927	3.610871	**2.375292**	4.113353	3.509645	2.827824	**2.012525**
	2	15.5646	13.21044	9.855803	**5.042138**	4.101196	3.366492	2.575467	**1.69059**	3.240194	2.753915	2.227466	**1.575288**
	2.5	10.8255	8.811944	5.982383	**2.637751**	3.251581	2.664732	2.041229	**1.353122**	2.725858	2.315012	1.889910	**1.322048**
	3	8.079715	6.312201	3.831586	**1.625216**	2.715753	2.246328	1.706166	**1.167302**	2.354605	2.055768	1.655120	**1.161476**
	4	5.088914	3.522501	1.747352	**1.062041**	2.11349	1.785838	1.263293	**1.023227**	2.003564	1.766636	1.261772	**1.023177**

Table 3.8: The Upper-Sided EWMA Zero-State ARL for Model 1, 2 and 3 with Different Head Starts ($\lambda = 0.05$)

Model		Model 1				Model 2				Model 3			
ϕ		1				0.9				0.9			
θ		0.9				0				0.5			
HS		0	25%	50%	75%	0	25%	50%	75%	0	25%	50%	75%
h		0.3937305	0.3948145	0.3981104	0.4075488	0.3937305	0.3948145	0.3981104	0.4075488	0.3937305	0.3948145	0.3981104	0.4075488
μ	0	399.9981	400	400	400	399.9981	400	400	400	399.9981	400	400	400
	0.1	393.7954	390.4383	383.2703	**367.9908**	363.1981	362.0194	359.7009	**353.0659**	330.346	328.3925	324.1525	**313.5379**
	0.2	385.9774	378.4052	362.6487	**332.0125**	330.4162	328.329	323.8963	**311.7418**	274.7572	271.3688	263.9015	**246.2034**
	0.3	376.0724	363.2015	337.9034	**292.9148**	301.1113	298.2062	291.9433	**275.1543**	230.1056	225.5629	215.7532	**193.5718**
	0.4	363.6287	344.439	309.1993	**251.9722**	274.8775	271.2358	263.3927	**242.7373**	194.0348	188.5659	177.105	**152.3728**
	0.5	348.3569	322.0659	277.2699	**211.1135**	251.3612	247.0569	237.8557	**214.0163**	164.7222	158.5155	145.9441	**120.0764**
	1	226.7233	171.2652	109.8308	**55.21723**	164.8451	158.1247	144.6589	**112.496**	79.67229	71.73983	58.39534	**37.11902**
	1.5	86.33647	48.16188	21.83434	**7.702441**	112.4883	104.4566	89.46617	**57.04604**	43.61337	35.90421	25.10152	**12.04917**
	2	15.66478	7.99541	4.110909	**2.063106**	79.48576	70.88435	55.83847	**27.41697**	25.90436	19.27798	11.52215	**4.45871**
	2.5	5.284412	3.714812	2.564866	**1.517672**	57.82297	49.14488	34.80101	**12.38766**	16.19567	10.91327	5.780521	**2.148705**
	3	3.777445	2.887928	2.103368	**1.267915**	43.04917	34.60327	21.35481	**5.381615**	10.49245	6.527346	3.325848	**1.412173**
	4	2.712547	2.15987	1.581696	**1.047583**	25.03684	17.47181	7.239994	**1.423399**	4.920408	3.000387	1.71872	**1.052313**

Table 3.9: The Upper-Sided EWMA Zero-State ARL for Model 4, 5 and 6 with Different Head Starts ($\lambda = 0.05$)

Model		Model 4				Model 5				Model 6			
ϕ		0.5				0.5				0.2			
θ		-0.5				0.5				0.5			
HS		0	25%	50%	75%	0	25%	50%	75%	0	25%	50%	75%
h		0.3937305	0.3948145	0.3981104	0.4075488	0.3937305	0.3948145	0.3981104	0.4075488	0.3937305	0.3948145	0.3981104	0.4075488
μ	0	399.9288	400	400	400	399.9288	400	400	400	399.9288	400	400	400
	0.1	292.4858	290.4142	285.9446	**275.8707**	166.6738	163.2194	155.8264	**141.6447**	108.1894	104.6224	97.32586	**84.58998**
	0.2	218.3747	215.1458	208.2016	**193.4564**	83.8276	79.93818	72.44883	**59.91337**	46.00022	42.75051	37.04398	**28.66493**
	0.3	166.5072	162.5935	154.4523	**138.0425**	49.80223	46.14085	39.81238	**30.35281**	26.73384	24.02218	19.82341	**14.3162**
	0.4	129.6447	125.3467	116.7663	**100.3027**	33.62803	30.31924	25.1223	**18.00454**	18.56032	16.2795	13.06446	**9.118547**
	0.5	103.0238	98.53401	89.95522	**74.24645**	24.85871	21.89257	17.59305	**12.07121**	14.24554	12.29025	9.716853	**6.67562**
	1	42.57685	38.31314	31.70229	**21.65283**	10.45573	8.628691	6.504167	**4.121855**	6.924856	5.79614	4.519356	**3.076785**
	1.5	24.01777	20.44023	15.67279	**9.10707**	6.64279	5.369338	3.994978	**2.506545**	4.819495	4.019002	3.145731	**2.154942**
	2	16.06048	13.10797	9.510294	**4.750671**	4.912898	3.948051	2.937662	**1.845717**	3.807826	3.183102	2.501685	**1.718154**
	2.5	11.80882	9.34935	6.467845	**2.789405**	3.93344	3.159282	2.369754	**1.485042**	3.209715	2.684281	2.135751	**1.446575**
	3	9.20281	7.117215	4.662643	**1.806005**	3.310067	2.653991	2.026332	**1.260337**	2.83244	2.322926	1.920798	**1.252417**
	4	6.205084	4.613449	2.531582	**1.11139**	2.537577	2.08917	1.574083	**1.047426**	2.207273	1.996197	1.568147	**1.047348**

Figure 3.2: Zero-State ARL for the Upper-Sided EWMA ($\lambda = 0.2$) with FIR

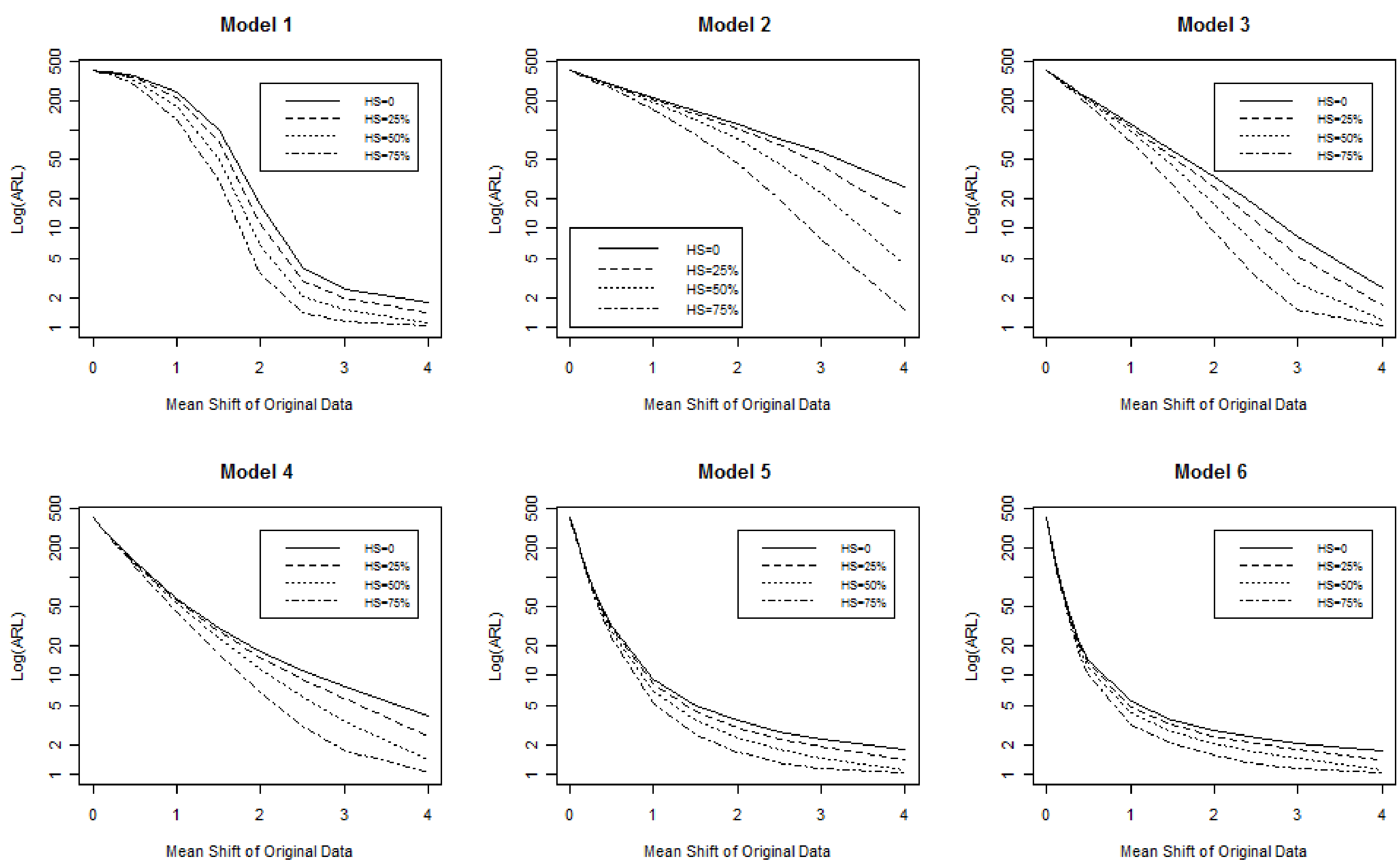

Figure 3.3: Zero-State ARL for the Upper-Sided EWMA ($\lambda = 0.1$) with FIR

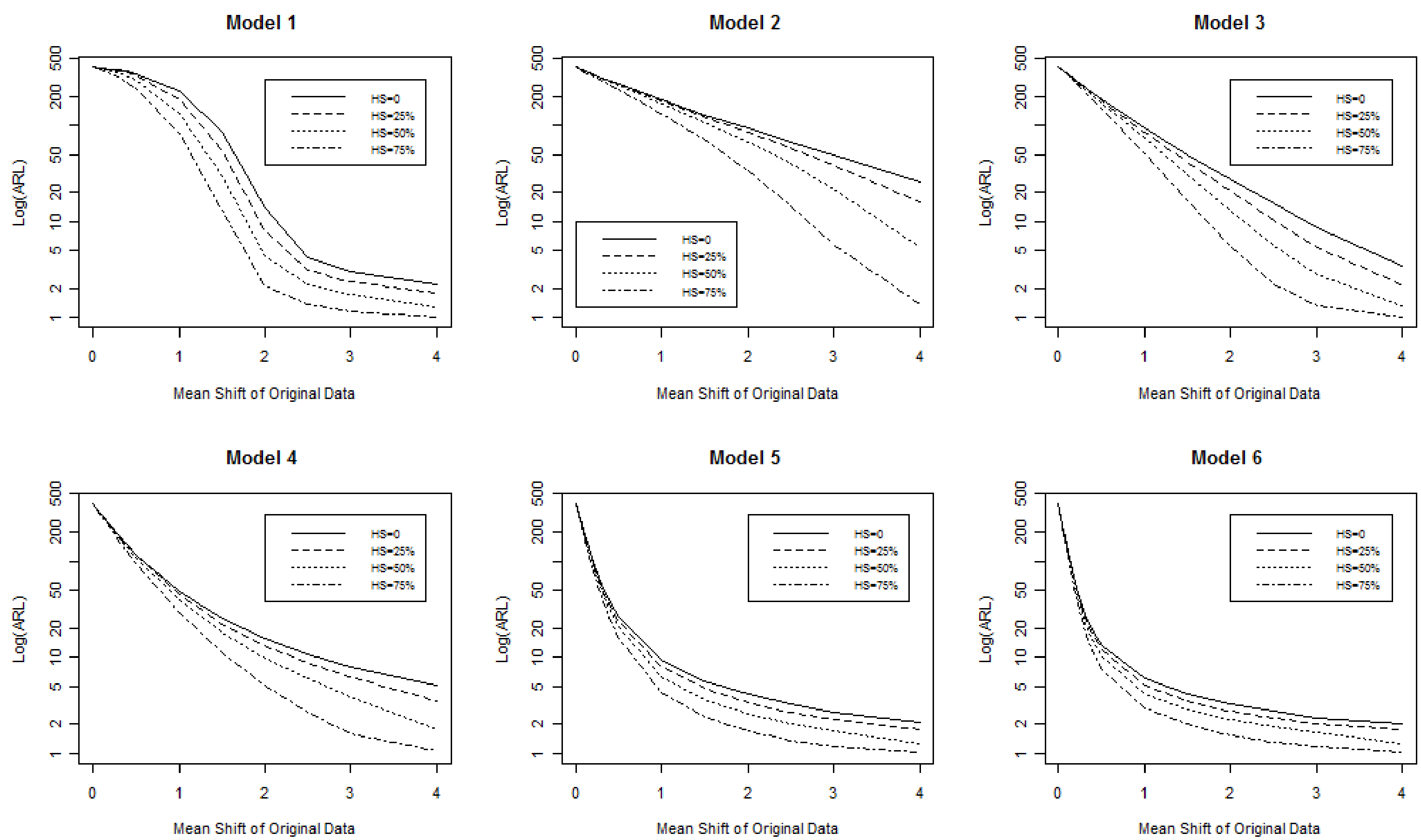

Figure 3.4: Zero-State ARL for the Upper-Sided EWMA ($\lambda = 0.05$) with FIR

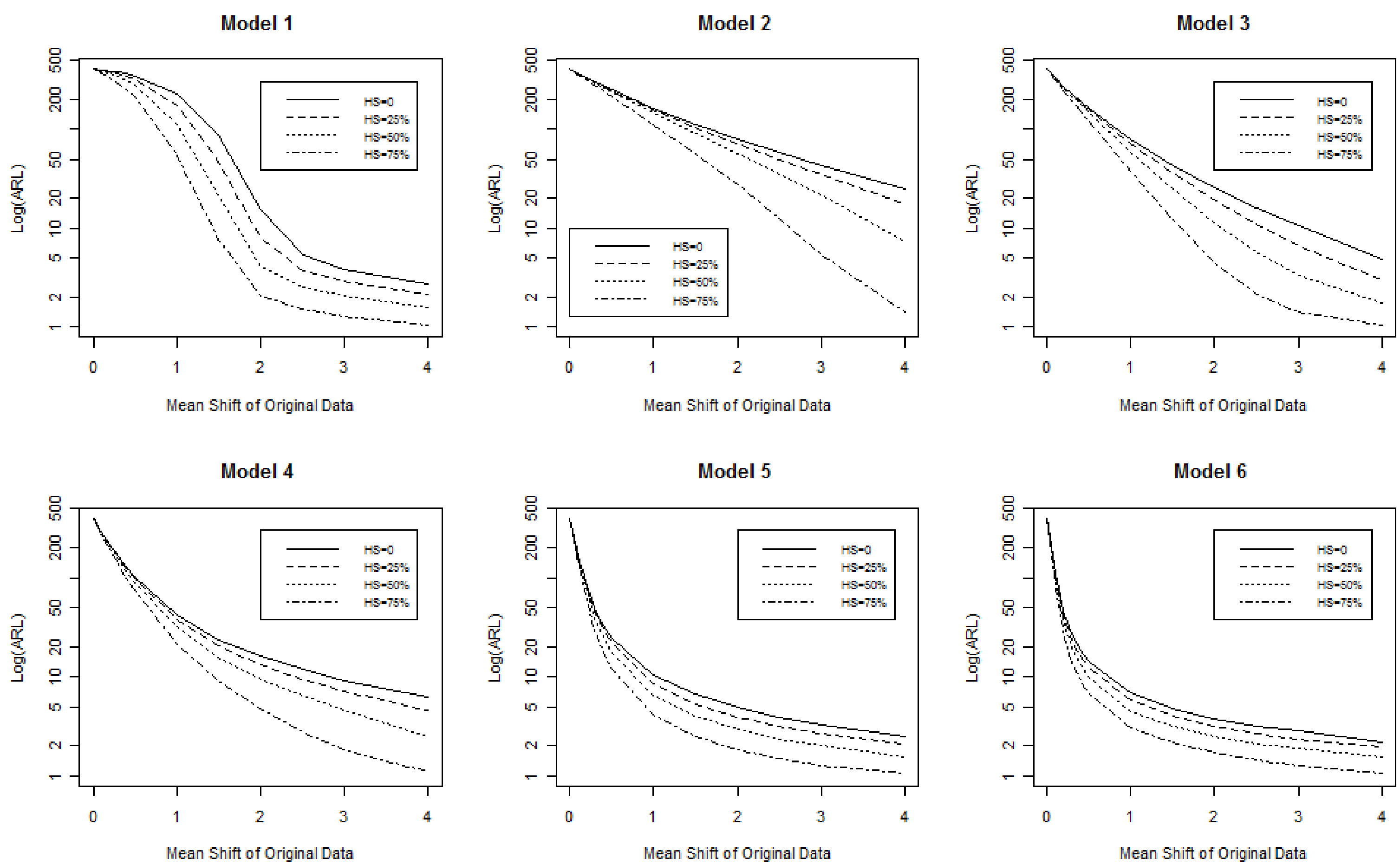

Chapter 4

Comparing the Upper-Sided EWMA with the Weighted CUSUM

As mentioned in Chapter 2, the WCUSUM has many advantages over other methods in detecting dynamic mean shifts. However, the WCUSUM also has its own flaws in some respects, and the upper-sided EWMA is comparable and in many instances better than the WCUSUM. The following sections will discuss them in detail. In addition, an improved Monte Carlo simulation approach is developed for the WCUSUM.

4.1 The Weighted CUSUM Scheme

Based on equations (2.4) and (2.5), Shu, Jiang and Tsui (2008) developed an algorithm based on a bivariate Markov chain for calculation of ARLs. It takes the random vector $(W_t,\, Q_t)'$ as a bivariate Markov chain, and the region $(0 \le W_t \le h,$ $-\infty < Q_t < \infty)$ or $(0 \le W_t \le h,\, -L \le Q_t \le L)$ will be divided into a large enough number of subregions to construct the transient states of a Markov chain and associated transition probability. L is chosen to be

$$L = 8\sqrt{\frac{\lambda}{2-\lambda}}$$

designed to cover nearly all the area under the distribution for Q_t. Specifically, $(0, h)$ is divided into m subintervals and $(-L, L)$ is divided into n subintervals, this results in the region $(0 \le W_t \le h,\, -L \le Q_t \le L)$ being divided into mn subregions or rectangles. The number $mn \times mn$ is the dimension of Markov chain transition probability matrix. Even if m and n are small or moderate, the problem with this approach is that mn could be an unacceptable large number for the dimension of a matrix to calculate the ARL by the non-homogeneous Markov chain equation (B.5). As discussed in Appendix B, equation (B.5) requires many transition matrix calculations and the large dimension for the transition probability matrix will take a long time to compute the ARL. Thus, it is very time consuming to use the Markov chain approach to compute the WCUSUM ARL for dynamic mean shift models (Luceño, 1999), which is a critical issue of the WCUSUM method. The Monte Carlo simulation approach is an alternative to compute the WCUSUM ARL.

4.2 Zero-State ARL Comparison

As discussed before, the upper-sided EWMA with FIR exhibits high performance in detecting dynamic mean shifts. Tables 4.1 and 4.2 show the zero-state ARL results for the upper-sided EWMA and the WCUSUM. Each table contains the results for three different models, two λ values 0.2 and 0.05, each with two head start values 0% and 75% for upper-sided EWMA; while one λ value 0.2 for WCUSUM. Shu, Jiang and Tsui (2008) pointed out that the optimal k value for the performance of the WCUSUM chart at a particular mean shift is nearly insensitive to the value of λ. Hence, the WCUSUM yields similar performance when $\lambda = 0.2$ and $\lambda = 0.05$. However, for the upper-sided EWMA, the λ has a greater effect on its performance. Figure 3.1 illustrates the effect of λ, in essence, smaller λ has a better performance for small and moderate dynamic mean shifts. It implies that $\lambda = 0.05$ is preferable to $\lambda = 0.2$ when detecting small or moderate dynamic mean shifts.

Figure 4.1 is a graphical representation of Tables 4.1 and 4.2. In Figure 4.1, EWMA 0.2 represents the upper-sided EWMA with $\lambda = 0.2$ and $HS = 0$, while EWMA 0.2a represents the upper-sided EWMA with $\lambda = 0.2$ and $HS = 75\%$. Similarly, EWMA 0.05 and EWMA 0.05a represent the upper-sided EWMA with $\lambda = 0.05$ and $HS = 0$ and the upper-sided EWMA with $\lambda = 0.05$ and $HS = 75\%$, respectively. The best ARL values are in dark font. The main trends noted from the tables and figures are as follow.

(1) The upper-sided EWMA with FIR feature $HS = 75\%$ is better than the WCUSUM for all six models and is much better when $\lambda = 0.05$. However, the WCUSUM exhibits a tiny advantage over the upper-sided EWMA without the FIR feature.

(2) For Model 1, the upper-sided EWMA with FIR feature $HS = 75\%$ displays much better performance than the WCUSUM while the small λ without the FIR feature does not show strong improvement. This particular case is very difficult for other methods to detect the mean drift and the upper-sided EWMA

with the FIR feature demonstrates its superiority over others.

(3) For models 5 and 6, which do not exhibit forecast recovery, the upper-sided EWMA with FIR feature also performs well while the WCUSUM deteriorates a little showing a similar performance to the traditional CUSUM (Shu, Jiang and Tsui, 2008).

4.3 Steady-State ARL Comparison

The steady-state ARL considers situations where the mean shift occurs at time τ while the process is in-control before time τ. we consider specifically the situation where the process goes through 40 in-control periods before a mean shift occurs. Note that the EWMA's FIR features do not work well in the steady-state situation because at the beginning the process is in control and any jump out of the control limit within the on-target time periods indicate a "false alarm". Table 4.3 shows the steady-state ARL data of the WCUSUM and the one-sided EWMAs. It contains the results for six different models, two λ values 0.2 and 0.05 for the upper-sided EWMA and one λ value 0.2 for the WCUSUM. The better ARL values are in dark font. Figure 4.2 is a graphic representation of the results in Table 4.3. We notice the following trends:

(1) For Model 1, 3 and 4, the upper-sided EWMA displays better performance with $\lambda = 0.05$ but worse with $\lambda = 0.2$ than the WCUSUM when the mean shifts are small and moderate. Opposing trends are seen when the mean shifts are large.

(2) For Model 2, the performance of the upper-sided EWMA with $\lambda = 0.05$ is better than the WCUSUM when the mean shifts are small and moderate. The

Figure 4.1: Zero-State ARL Comparisons Between the Upper-Sided EWMA and the WCUSUM for Six Models

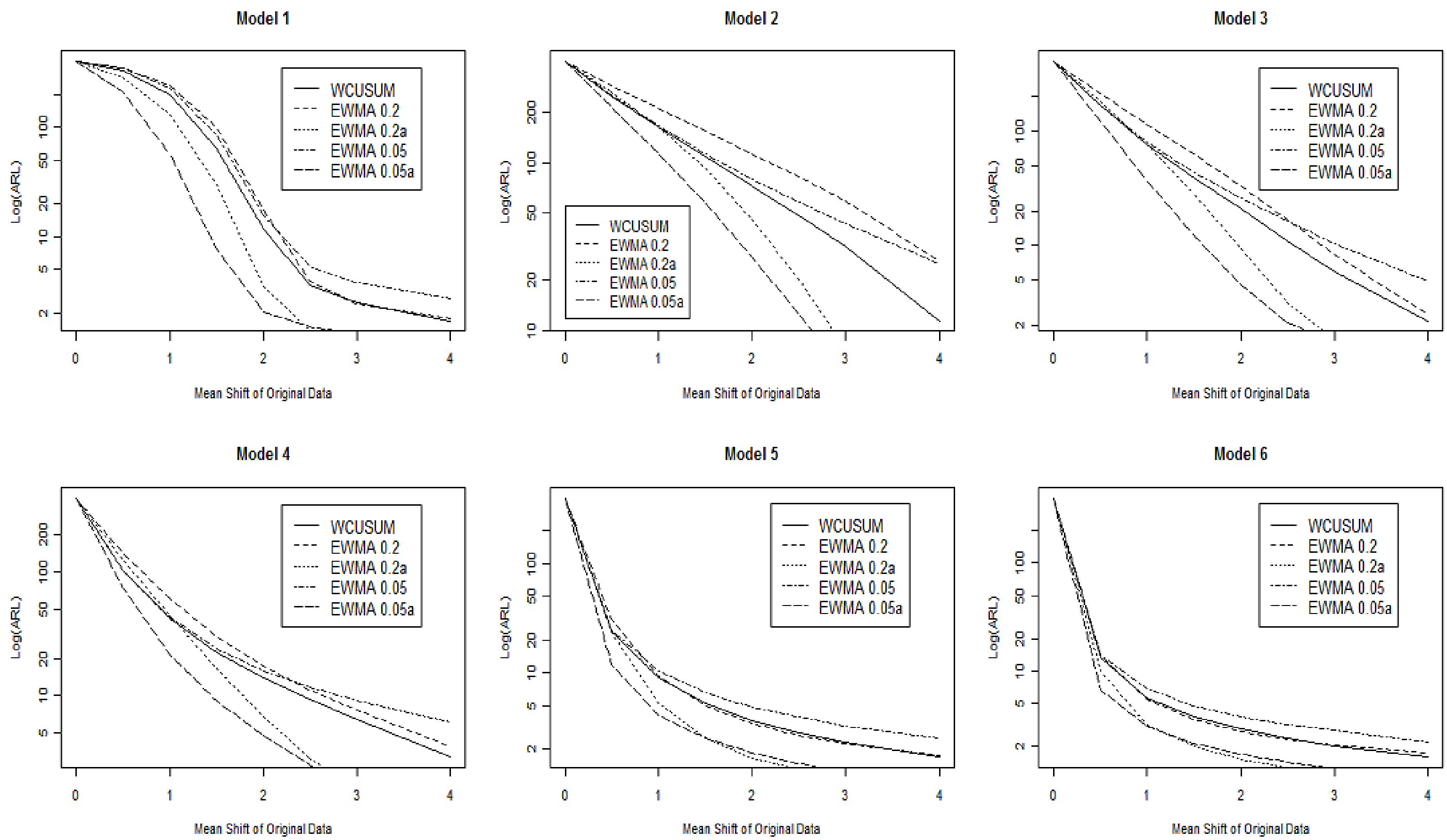

Table 4.1: Zero-State ARL Comparisons Between the Upper-Sided EWMA and the WCUSUM for Models 1, 2 and 3

				One-sided EWMA				WCUSUM
				$\lambda = 0.2$		$\lambda = 0.05$		$\lambda = 0.2$
				h=0.930427	h=0.9403742	h=0.3937305	h=0.4075488	h=2.009
ϕ	θ	FS_∞	μ	HS=0	HS=75%	HS=0	HS=75%	
			0	400	400	400	400	400
1.0	0.9	0.0	0.5	352.4097	287.453	348.3569	**211.1135**	334.7
			1	239.727	129.3926	226.7233	**55.21723**	197.1
			1.5	99.4664	29.90202	86.33647	**7.702441**	63.9
			2	17.30417	3.479821	15.66478	**2.063106**	11.9
			2.5	3.97578	1.398912	5.284412	**1.517672**	3.6
			3	2.453088	1.146115	3.777445	**1.267915**	2.5
			4	1.791267	1.016936	2.712547	**1.047583**	1.7
0.9	0.0	0.1	0.5	288.8332	262.9347	251.3612	**214.0163**	250.9
			1	210.5637	162.6172	164.8451	**112.496**	163
			1.5	154.5738	91.744	112.4883	**57.04604**	108
			2	113.5214	45.82721	79.48576	**27.41697**	72.8
			2.5	82.98712	20.09532	57.82297	**12.38766**	48.5
			3	59.33347	7.839003	43.04917	**5.381615**	31.6
			4	26.0654	1.495663	25.03684	**1.423399**	11.4
0.9	0.5	0.2	0.5	210.1853	181.6803	164.7222	**120.0764**	163.4
			1	113.8846	75.80774	79.67229	**37.11902**	76.2
			1.5	62.12573	28.00715	43.61337	**12.04917**	39.1
			2	33.08922	9.253565	25.90436	**4.45871**	20.7
			2.5	16.85081	3.136022	16.19567	**2.148705**	11
			3	8.313846	1.488639	10.49245	**1.412173**	5.9
			4	2.52289	1.023507	4.920408	**1.052313**	2.2

WCUSUM is better for other situations.

(3) For models 5 and 6, which do not have forecast recovery situations, the performances are very close when the mean shifts occur at small magnitudes while

Table 4.2: Zero-State ARL Comparisons Between the Upper-Sided EWMA and the WCUSUM for Models 4, 5 and 6

				One-sided EWMA				WCUSUM
				$\lambda = 0.2$		$\lambda = 0.05$		$\lambda = 0.2$
				h=0.930427	h=0.9403742	h=0.3937305	h=0.4075488	h=2.009
ϕ	θ	FS_∞	μ	HS=0	HS=75%	HS=0	HS=75%	
			0	400	400	400	400	400
0.5	-0.5	0.3	0.5	143.8591	127.2918	103.0238	**74.24645**	102.5
			1	60.92744	44.15928	42.57685	**21.65283**	41.7
			1.5	30.41559	16.63105	24.01777	**9.10707**	22.5
			2	17.49545	6.799724	16.06048	**4.750671**	14.1
			2.5	11.19824	3.106699	11.80882	**2.789405**	9.4
			3	7.692241	1.713781	9.20281	**1.806005**	6.5
			4	3.943643	1.056462	6.205084	**1.11139**	3.2
0.5	0.5	1.0	0.5	31.30606	23.6089	24.85871	**12.07121**	24.4
			1	9.224577	5.234984	10.45573	**4.121855**	9.1
			1.5	5.036461	2.509976	6.64279	**2.506545**	5.3
			2	3.490132	1.676099	4.912898	**1.845717**	3.7
			2.5	2.712429	1.315492	3.93344	**1.485042**	2.8
			3	2.260535	1.138218	3.310067	**1.260337**	2.3
			4	1.766223	1.016806	2.537577	**1.047426**	1.7
0.2	0.5	1.6	0.5	14.17267	9.985868	14.24554	**6.67562**	13.3
			1	5.411293	3.219155	6.924856	**3.076785**	5.7
			1.5	3.570137	2.013054	4.819495	**2.154942**	3.8
			2	2.771038	1.532465	3.807826	**1.718154**	2.9
			2.5	2.317208	1.278214	3.209715	**1.446575**	2.4
			3	2.050167	1.131147	2.83244	**1.252417**	2
			4	1.744554	1.01674	2.207273	**1.047348**	1.6

the upper-sided EWMA with $\lambda = 0.2$ performs a bit better for moderate or large shifts.

4.4 Improved Monte Carlo Simulation for the WCUSUM Scheme

As discussed before, the Markov chain approach is extremely difficult to use for calculating the WCUSUM ARL in dynamic mean shift situations. A simple alternative is Monte Carlo simulation, which is a popular approach to evaluate the performance of statistical methods. Its advantage is simple and easy to explain, but one of the big issues is having to do large amounts of calculations. Thus, finding an efficient way is critical for some cases. The details of how to simulate WCUSUM ARL are presented in Appendix C.

From Appendix C, it is easy to see that every single simulation of run length should be efficient, otherwise the $160,000$ simulations will be take an unfeasibly long time to yield the average run length. The challenge of simulating the run length algorithm is how to efficiently calculate the weight vector $\boldsymbol{Q}$ since the dimension n usually is large. Here, a new method is proposed to reduce matrix dimension from $n \times n$ to $m \times m$, where $n = km$, m is an efficient dimension number for computer processing.

From Equation (C.2)

$$\boldsymbol{Q} = \boldsymbol{Y}_{n\times n}\boldsymbol{\lambda},$$

Table 4.3: Steady-State ARL Comparisons Between the Upper-Sided EWMA and the WCUSUM for Six Models

Model		Model 1			Model 2			Model 3		
		One-sided EWMA		WCUSUM	One-sided EWMA		WCUSUM	One-sided EWMA		WCUSUM
λ		0.2	0.05	0.2	0.2	0.05	0.2	0.2	0.05	0.2
h		0.930427	0.3937305	3.383	0.930427	0.3937305	3.383	0.930427	0.3937305	3.383
μ	0	361.525	**360.8199**	389.1	361.525	**360.8199**	389.1	361.525	**360.8199**	389.1
	0.5	307.4233	**284.2241**	309.9	258.1912	**221.4896**	240.5	186.2134	**141.5156**	154.1
	1	193.4509	**154.1901**	174	184.6292	**140.6714**	153	97.01769	**63.60538**	69.4
	1.5	72.12792	**48.18069**	56.1	131.3573	**92.2242**	99.2	49.81465	**31.97808**	35.1
	2	11.39001	**8.470314**	11.2	91.99233	**62.19183**	65.2	24.60886	**17.50139**	18.5
	2.5	**2.865285**	3.564228	3.6	63.04714	42.95776	**42.7**	11.63671	10.23278	**10.1**
	3	**1.889285**	2.71029	2.4	41.57248	30.25333	**27.7**	**5.468904**	6.353128	5.7
	4	**1.376198**	2.000579	1.6	15.28379	15.6194	**10.7**	**1.749116**	3.008357	2.2
Model		Model 4			Model 5			Model 6		
μ	0	361.525	**360.8199**	389.1	361.525	**360.8199**	389.1	361.525	**360.8199**	389.1
	0.5	128.0755	**88.3972**	96.7	27.10789	**19.7694**	22.4	12.11316	**11.18322**	12.4
	1	52.8268	**34.36094**	38.3	**7.583433**	7.897336	8.5	**4.469711**	5.327316	5.4
	1.5	25.39184	**18.41578**	20.4	**4.030326**	4.945195	4.9	**2.913711**	3.703818	3.6
	2	13.94123	**11.86281**	12.7	**2.76324**	3.646684	3.5	**2.25202**	2.934077	2.7
	2.5	**8.468893**	8.480952	8.5	**2.140208**	2.92419	2.7	**1.883856**	2.480741	2.3
	3	**5.508479**	6.456894	5.9	**1.778255**	2.467274	2.2	**1.65806**	2.178219	2
	4	**2.600968**	4.170063	3	**1.364145**	1.918307	1.6	**1.354265**	1.779786	1.6

Figure 4.2: Steady-State ARL Comparisons Between the Upper-Sided EWMA and the WCUSUM for Six Models

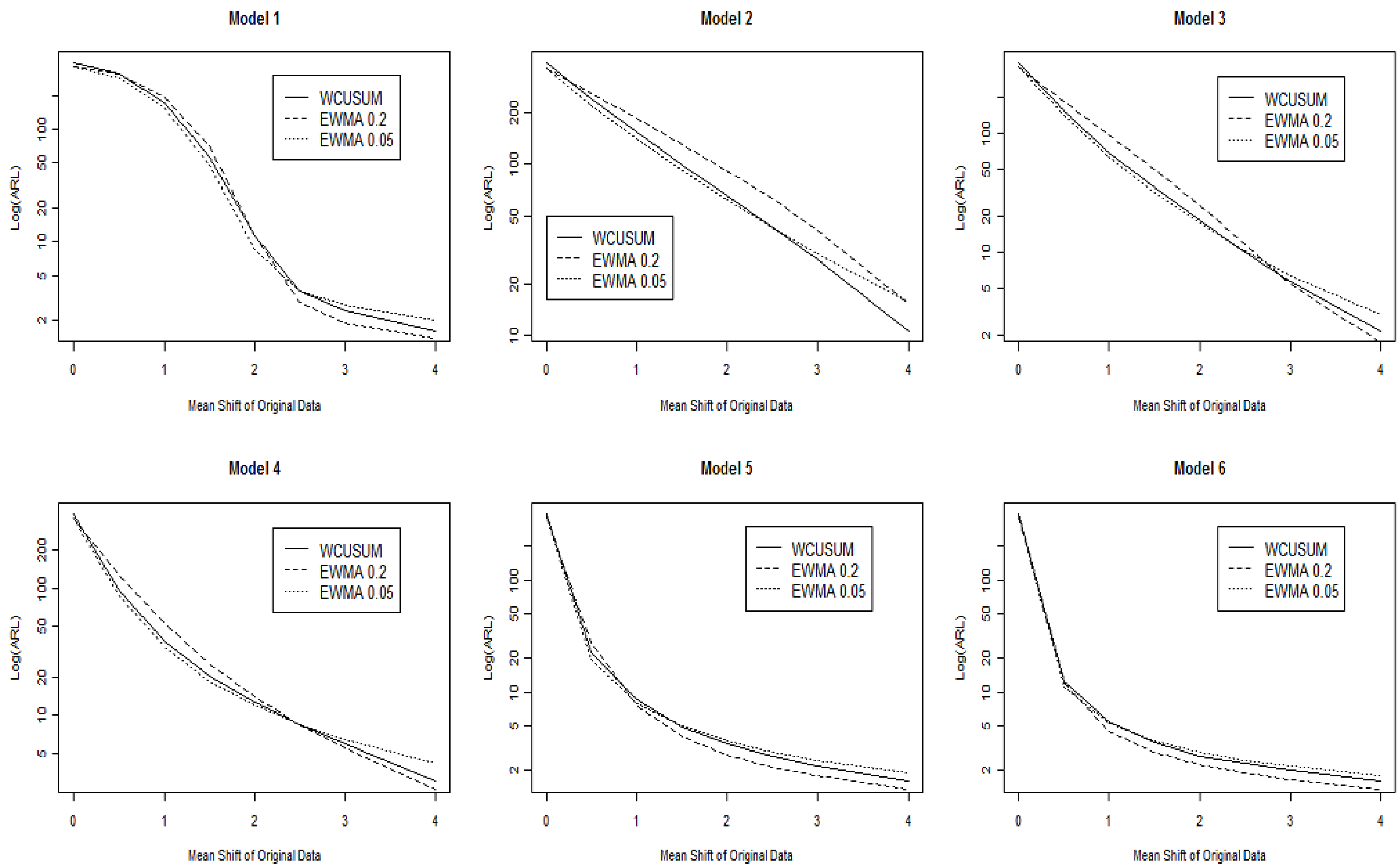

it is easy to see that the entries of vector $\boldsymbol{\lambda}$ have an interesting pattern, which is

$$\lambda_{i+m} = \lambda_i(1-\lambda)^m.$$

Divide the n dimension vector $\boldsymbol{\lambda}$ into k sub-vectors with dimension m, $n = km$, then $\boldsymbol{\lambda}$ can be presented as

$$\boldsymbol{\lambda} = \{\boldsymbol{\lambda}_1, \boldsymbol{\lambda}_2, \cdots, \boldsymbol{\lambda}_k\}',$$

where m dimension vectors $\boldsymbol{\lambda}_i$ and $\boldsymbol{\lambda}_{i+1}$ have the following relationship

$$\boldsymbol{\lambda}_{i+1} = \boldsymbol{\lambda}_i(1-\lambda)^m, \qquad i = 1, 2, \cdots, k-1$$

or

$$\lambda_{i+1,j} = \lambda_{i,j}(1-\lambda)^m, \qquad i = 1, 2, \cdots, k-1; \qquad j = 1, 2, \cdots, m.$$

Similarly, the n dimension vector $\boldsymbol{Q}$ can be presented as

$$\boldsymbol{Q} = \{\boldsymbol{Q}_1, \boldsymbol{Q}_2, \cdots, \boldsymbol{Q}_k\}'$$

and the n dimension vector $\mathbf{Y}$ can be presented as

$$\boldsymbol{Y} = \{\boldsymbol{Y}_0, \boldsymbol{Y}_1, \boldsymbol{Y}_2, \cdots, \boldsymbol{Y}_{k-1}\}'$$

where

$$\boldsymbol{Y}_i = \{y_{im+1}, y_{im+2}, \cdots, y_{im+m}\}, \qquad i = 0, 1, 2, \cdots, k-1.$$

In addition, we define vector $\boldsymbol{Y}_{ij}$ as

$$\boldsymbol{Y}_{ij} = \{y_{im+j}, y_{im+j-1}, \cdots, y_{im+j-m+1}\}, \qquad i = 1, 2, \cdots, k-1; \qquad j = 1, 2, \cdots, m;$$

sub-matrix $\boldsymbol{Y}_{i(m\times m)}$ as

$$\boldsymbol{Y}_{i(m\times m)} = \{\boldsymbol{Y}_{i1}, \boldsymbol{Y}_{i2}, \cdots, \boldsymbol{Y}_{im}\}', \qquad i = 1, 2, \cdots, k-1$$

and sub-matrix $\boldsymbol{Y}_{m\times m}$ as

$$\boldsymbol{Y}_{m\times m} = \begin{pmatrix} y_1 & 0 & 0 & \cdots & 0 & 0 \\ y_2 & y_1 & 0 & \cdots & 0 & 0 \\ \cdot & \cdot & \cdot & \cdots & 0 & 0 \\ \cdot & \cdot & \cdot & \cdots & 0 & 0 \\ \cdot & \cdot & \cdot & \cdots & y_1 & 0 \\ y_m & y_{m-1} & y_{m-2} & \cdots & y_2 & y_1 \end{pmatrix}$$

Hence, $\boldsymbol{Q}_1$ is

$$\boldsymbol{Q}_1 = \boldsymbol{Y}_{m\times m}\boldsymbol{\lambda}_1$$

and $\boldsymbol{Q}_i$ can be presented as

$$\boldsymbol{Q}_i = \boldsymbol{Q}_{i-1}(1-\lambda)^m + \boldsymbol{Y}_{(i-1)(m\times m)}\boldsymbol{\lambda}_1, \qquad i = 2, 3, \cdots, k.$$

The above algorithm only involves in $m \times m$ dimension matrix calculations. Thus, it is highly efficient by greatly reducing the amount of calculation for simulation.

Table 4.4 displays the simulation results of the WCUSUM created by the improved Monte Carlo simulation algorithm, which are very close to the results of Shu, Jiang and Tsui(2008).

Table 4.4: Simulated Zero-State ARL of the WCUSUM ($\lambda = 0.2$)

Model		Model 1	Model 2	Model 3	Model 4	Model 5	Model 6
ϕ		1	0.9	0.9	0.5	0.5	0.2
θ		0.9	0	0.5	-0.5	0.5	0.5
μ	0	400	400	400	400	400	400
	0.5	335.5191	251.6611	163.8554	103.0101	24.40665	13.321
	1	196.6326	162.7646	76.37638	41.0622	9.15385	5.7194
	1.5	60.49983	107.9981	39.09337	22.4485	5.2855	3.77415
	2	10.58418	72.70316	20.76481	14.0128	3.6591	2.8822
	2.5	3.549444	48.48518	11.07029	9.4156	2.81585	2.37095
	3	2.470769	31.52063	5.955244	6.4805	2.2881	2.03915
	4	1.705362	11.42681	2.193763	3.22745	1.68	1.64995

Chapter 5

Monitoring Molecular Weight in a Polymer Manufacturing Process

Polymer molecular weight is a key quantity that determines many physical properties. Temperatures for transitions from liquids to waxes to rubbers to solids are examples. But also important mechanical properties such as stiffness, strength, viscoelasticity, toughness and viscosity. For instance, it is well known that polymer strength (S) increases with molecular weight (M) through the functional equation

$$S = S_\infty - \frac{A}{M},$$

where S_∞ is the ceiling strength and A is a constant. For a polymer to be useful, it must have mechanical properties sufficient to bear design loads. In polymer manufacturing, molecular weight is one of the key quality indicators monitored.

In this chapter we examine molecular weight data from a polymer manufacturing process and illustrate all the steps involved in setting up control charts to monitor the mean molecular weight. The analysis begins with an exploration of the available

Table 5.1: Polymer Molecular Weights from Montgomery (2005, p. 482)

2048	2025	2017	1995	1983	1943	1940	1947	1972	1983	1935	1948
1966	1954	1970	2039	2015	2021	2010	2012	2003	1979	2006	2042
2000	2002	2010	1975	1983	2021	2051	2056	2018	2030	2023	2036
2019	2000	1986	1952	1988	2016	2002	2004	2018	2002	1967	1994
2001	2013	2016	2019	2036	2015	2032	2016	2000	1988	2010	2015
2029	2019	2016	2010	2006	2009	1990	1986	1947	1958	1983	2010
2000	2015	2032									

data to establish the extent of autocorrelation. Once any problematic observations are removed, the data are taken to be as Phase I Data produced under on-target operation, and the model parameters are estimated and the charts calibrated. The estimated process parameters are then used to simulate data with out-of-control excursions to illustrate the use of the charts. Graphs and numerical results are reported to aid interpretation.

5.1 The Molecular Weight Data

Montgomery (2005, p. 482) reports molecular weight measurements from a polymer manufacturing process. In total, 75 measurements were collected on a polymer, measurements were gathered every 2 hours. The data are reproduced in Table 5.1 (read across from left to right, then down).

The top-left plot in Figure 5.1 contains a run plot of the data. No obvious unusual observations are noted. The clustering of neighboring observations looks somewhat stronger than for independent data. No apparent trend or seasonality is shown.

A scatter plot of x_t vs. x_{t-1} is displayed in the top-right plot of Figure 5.1. It is clear that consecutive molecular weights are positively correlated. A more thorough exploration of the correlation structure is shown in the bottom-left plot of Figure 5.1 where the autocorrelation function for the molecular weights is plotted for 18 lags. Only the two leading autocorrelations appear significant. Overall, the plot resembles a typical autocorrelation function for an autoregressive time series of order 1 with a positive coefficient.

5.2 ARIMA Fit and Residuals

Following the above preliminary findings, we began the modeling by fitting a low-order $ARIMA$ model to the x data, namely an $ARIMA(1,0,1)$ model. The fitting was done in SAS using the ARIMA procedure. No trend nor seasonality terms were added, only a mean term was included. The results of the fit are displayed in Table 5.2.

Table 5.2: Conditional Least Squares Estimation

Parameter	Estimate	Standard Error	t-value
Mu	2001.03	6.56614	305.32
MA1	-0.19009	0.16878	-1.13
AR1	0.57688	0.14245	4.05

Table 5.2 suggests that if an $ARIMA(1,0,1)$ was a good model for the molecular weight x data, then only the mean term and the autoregressive coefficient

Figure 5.1: Molecular Weight Data and Autocorrelation Plots

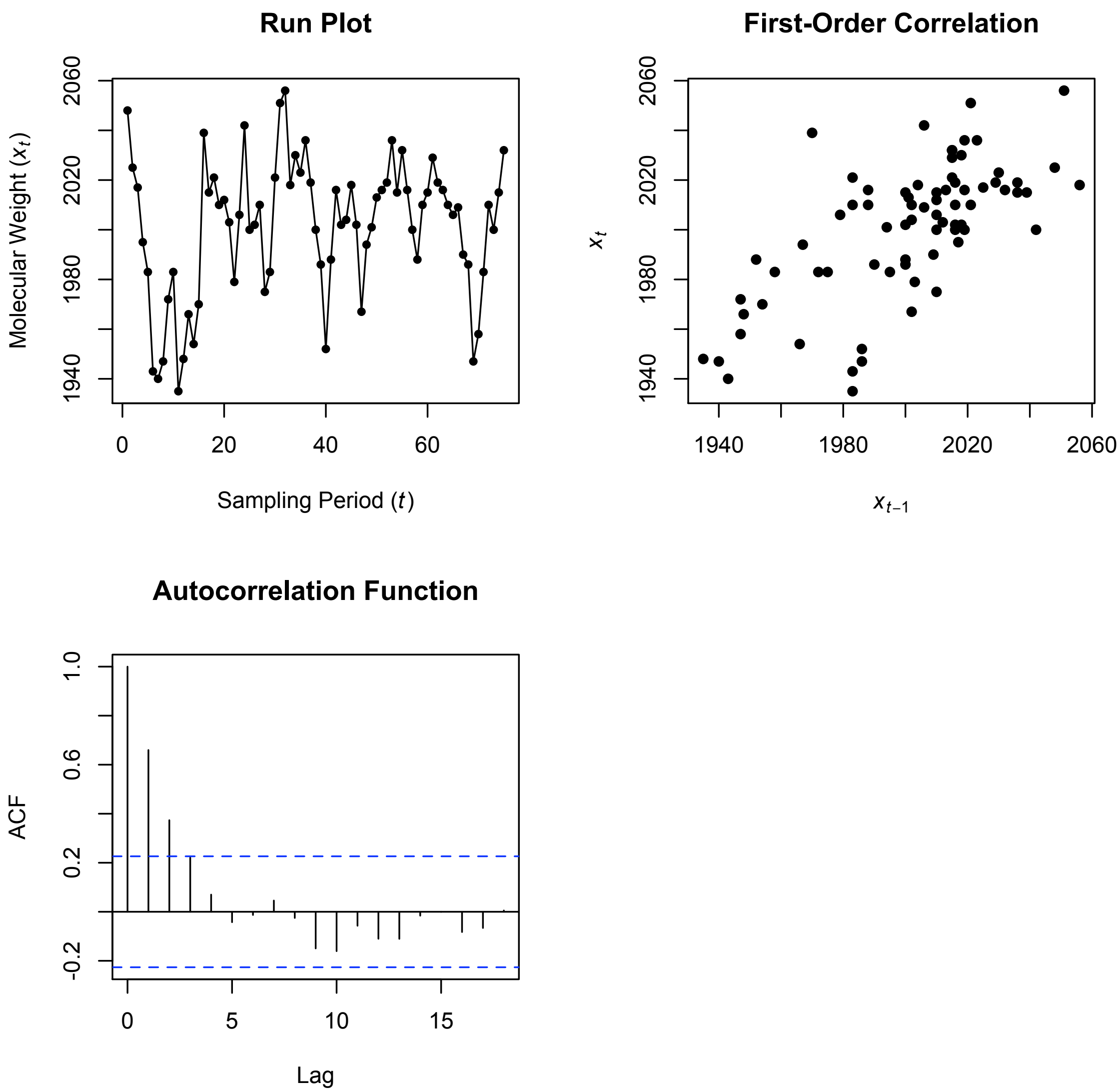

would be relevant. Let's examine further the goodness of fit of the model. Taking $\mu_0 = \overline{x} = 2001.03$, from equation (1.2), the residuals y_t from an $ARIMA(1,0,1)$ model with mean term μ_0 are given by

$$y_t = \frac{(1-B)^d\phi(B)}{\theta(B)}(x_t - \mu_0) = \frac{1-\phi B}{1-\theta B}(x_t - \mu_0)$$

$$= (x_t - \mu_0) + (\theta - \phi)(x_{t-1} - \mu_0) + \theta(\theta - \phi)(x_{t-2} - \mu_0) + \cdots + \theta^{n-1}(\theta - \phi)(x_{t-n} - \mu_0) + \cdots,$$

where ϕ and θ are the respective autoregressive and moving average coefficients. From Table 5.2, the t value associated with estimate θ is -1.13, which could not reject that θ equals 0. However, the conditional least squares estimation gives estimate θ as -0.19. Here we can consider that θ equals -0.19. Taking $\phi = 0.67688$ and $\theta = -0.19$ yields residuals

$$\begin{aligned} y_t &\approx (x_t - \mu_0) + (\theta - \phi)(x_{t-1} - \mu_0) + \theta(\theta - \phi)(x_{t-2} - \mu_0) \\ &= (x_t - 2001.03) - 0.76688(x_{t-1} - 2001.03) + 0.1457(x_{t-2} - 2001.03). \quad (5.1) \end{aligned}$$

The residuals were calculated using eqn. (5.1), and run and autocorrelation plots were produced, these are shown in Figure 5.2. Both plots suggest that the residuals are quite random, centered around 0, and that the $ARIMA(1,0,1)$ model effectively removed the autocorrelations. Note that the mean and standard deviation of the residuals are $\overline{y} = 0.2294$ and $s_y = 20.616$. To match the assumption of unit variance for the residuals made in the control charts discussed in previous chapters, we need to standardize the residuals to have a variance of 1, thus we just need to divide each residual by s_y. Thus the final transformation to work with from eqn.

Figure 5.2: Residual Plots from ARIMA(1,0,1) Fit

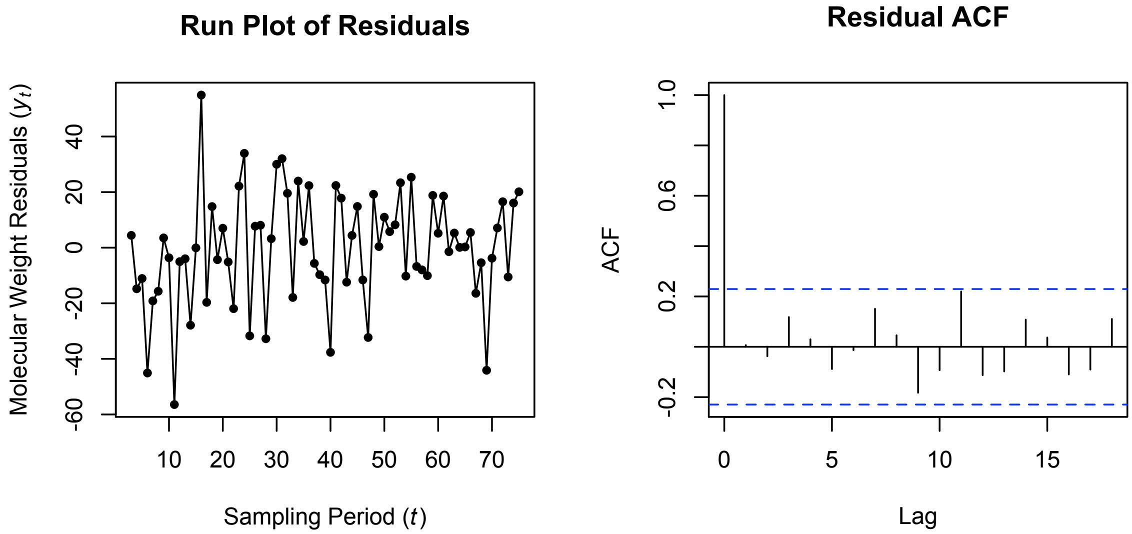

(5.1) is

$$y_t \approx \frac{1}{20.616}[(x_t - 2001.03) - 0.76688(x_{t-1} - 2001.03) + 0.1457(x_{t-2} - 2001.03)]. \tag{5.2}$$

As a final check on the residuals, a simple Shewhart chart of the residuals from (5.2), namely a plot of y_t vs. t, with control limits at $\pm 3\sigma_y = \pm 3$ is shown in Figure 5.3. No residual seems off-target. Thus we will assume that the 75 molecular weights came from in-control process operation.

5.3 Simulated Cases with Dynamic Mean Shifts

Based on equations (1.3) and (5.1) for the ARIMA model time series, a step mean shift in time series x_t could lead to dynamic mean shift in time series y_t. Time series $\{y_t\}$ values are approximately independent and we can randomly generate dynamic

Figure 5.3: Shewhart Chart Plot of the Residuals

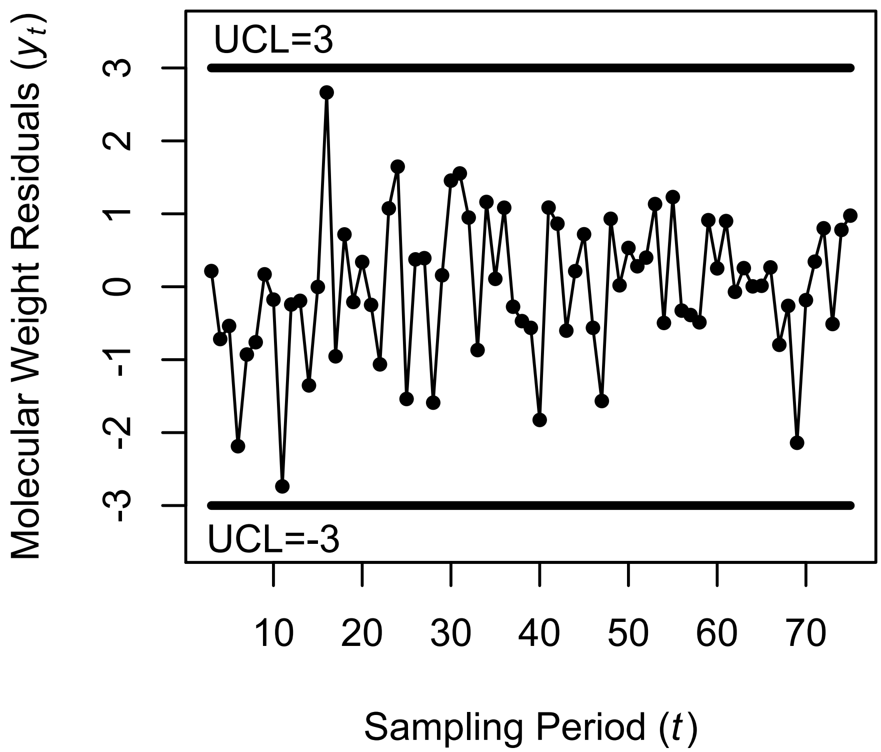

patterned means shift data to illustrate performance of some statistics that are used for detecting mean shift. In the illustrations below, the upper-sided EWMA statistic is based on equation (3.1), the WCUSUM statistic is based on equations (2.4) and (2.5) and the traditional CUSUM statistic is based on equation (2.1).

5.3.1 Performance Comparison of Zero-State Case

In this section, the charts are illustrated on a simulated data set of 200 x_t observations for which the mean changed from $\mu_0 = 0$ to $\mu = 1$ at the very beginning (zero state). The residual mean ξ_t were calculated from eqn. (1.4) with $\tau = 1$, $\mu = 0$, $\theta = -0.19$ and $\phi = 0.57688$. The 200 residual values y_t were generated in R with $\sigma_y = 1$. The first 13 values are displayed in column 2 of Figure 5.3.

The charts were then applied, specifically the upper-sided EWMA with FIR feature, the WCUSUM and traditional CUSUM schemes. Three head start leads were used, namely $HS = 0$, $HS = 50\%$ and $HS = 75\%$. The numerical chart values are displayed in columns $3 - 7$ of Table 5.3 along with the associated control limits for an $ARL_0 = 400$ and $\lambda = 0.1$ for the EWMA and $\lambda = 0.2$ for the WCUSUM. In this illustration, the traditional CUSUM detects the change at 13^{th} run, the WCUSM and the EWMA with $HS = 0\%$ detect the change at run 12, while the EWMA with $HS = 50\%$ and $HS = 75\%$ detect the change at run 11. The values in dark font in Table 5.3 indicate that the chart has gone beyond the control limit.

The charts values are plotted in Figure 5.4. The plots display graphically the features just noted. In this case, the higher the head start HS, the quicker the EWMA chart detects the change. Note also the case is no subtantive difference between the EWMA and the WCUSUM. The traditional CUSUM appears to be the slowest to

Table 5.3: Zero-State Simulated Data and the Responses of Upper-Sided EWMA, WCUSUM and CUSUM Statistics ($\mu = 1$, $\phi = 0.57688$, $\theta = -0.19$, $\sigma_y = 1$)

		Upper-Sided EWMA			WCUSUM	CUSUM
		$\lambda = 0.1$			$\lambda = 0.2$	
		h=0.60886	h=0.621	h=0.6125	h=3.383	h=4.173
t	Simulated y_t	HS=0	HS=75%	HS=50%		
1	0.6277	0.0628	0.4820	0.3384	0.0160	0.1277
2	0.3503	0.0915	0.4688	0.3396	0.0000	0.0000
3	0.0413	0.0865	0.4260	0.3098	0.0000	0.0000
4	1.4135	0.2192	0.5248	0.4201	0.3640	0.9135
5	-0.4609	0.1512	0.4262	0.3320	0.1463	0.0000
6	0.2965	0.1657	0.4132	0.3285	0.0973	0.0000
7	0.7640	0.2255	0.4483	0.3720	0.1885	0.2640
8	1.7341	0.3764	0.5769	0.5082	0.9573	1.4981
9	-0.3518	0.3036	0.4840	0.4222	0.5927	0.6463
10	1.6540	0.4386	0.6010	0.5454	1.3696	1.8002
11	1.6585	0.5606	**0.7068**	**0.6567**	2.3777	2.9587
12	1.5923	**0.6638**	**0.7953**	**0.7503**	**3.4861**	4.0510
13	1.3660	**0.7340**	**0.8524**	**0.8118**	**4.4257**	**4.9170**

react to the change, although not by much.

5.3.2 Performance Comparison of Steady-State Case

Similarly, a steady state data set was simulated corresponding to a situation where the mean for original x_t data shifts from $\mu_0 = 0$ to $\mu = 1$ at time $\tau = 41$. Thus the residual means ξ_t were calculated from eqn. (1.4) with $\mu = 1$, $\tau = 41$, $\theta = -0.19$ and $\phi = 0.57688$. In total 200 residuals were generated in R with the ξ_t means and $\sigma_y = 1$. Some of the data are listed in column 2 of Table (5.4). In this case, the upper-sided EWMA with $HS = 0\%$, the WCUSM and the traditional CUSUM were used. The

Figure 5.4: Zero-State Control Charts with Shift $\mu = 1$, $\sigma_y = 1$

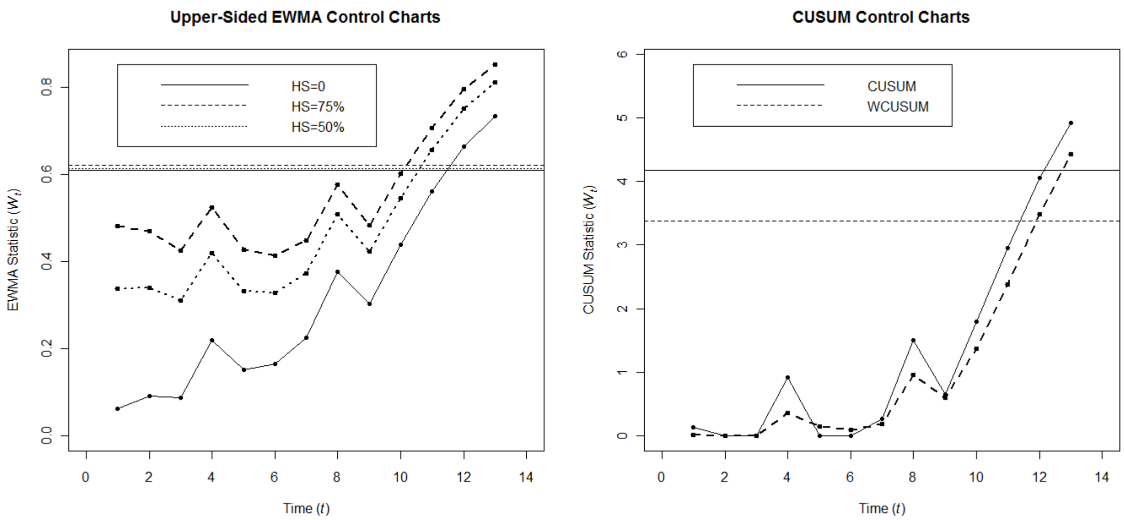

EWMA detects the change 14 runs after the change took place, while the WCUSUM and the traditional CUSUM react the change 15 runs after change. Thus the EWMA shows a slightly better performance for this data set. Figure 5.5 graphically presents the values of Table 3.4.

Table 5.4: Steady-State Simulated Data and the Responses of Upper-Sided EWMA, WCUSUM and CUSUM Statistics ($\mu = 1$, $\phi = 0.57688$, $\theta = -0.19$, $\sigma_y = 1$)

		Upper-Sided EWMA	WCUSUM	CUSUM
		$\lambda = 0.05$	$\lambda = 0.2$	
t	Simulated y_t	h=0.3937	h=3.383	h=4.173
1	0.1853	0.00926	0.0000	0.0000
.	.	.	.	.
.	.	.	.	.
.	.	.	.	.
31	-0.2782	0.0038	0.0000	0.0000
32	2.0850	0.1079	0.4545	1.5850
33	1.0463	0.1548	0.6942	2.1313
34	0.6477	0.1794	0.7651	2.2790
35	0.1359	0.1772	0.6153	1.9149
36	-0.5003	0.1434	0.3860	0.9146
37	0.3177	0.1521	0.3410	0.7323
38	0.9413	0.1915	0.5113	1.1736
39	0.2816	0.1960	0.4316	0.9552
40	0.0958	0.1910	0.3058	0.5510
41	1.3191	0.2474	0.7258	1.3701
42	-1.7275	0.1487	0.5817	0.0000
43	-0.0128	0.1406	0.5565	0.0000
44	1.1979	0.1935	0.7512	0.6979
45	-0.0921	0.1792	0.6300	0.1058
46	1.1892	0.2297	0.9067	0.7950
47	0.6140	0.2489	0.9574	0.9090
48	-0.3290	0.2200	0.7174	0.0799
49	0.1536	0.2167	0.6265	0.0000
50	1.3152	0.2716	1.0120	0.8152
51	1.4027	0.3282	1.6067	1.7179
52	0.0920	0.3164	1.3842	1.3099
53	1.0265	0.3519	1.7220	1.8364
54	1.5117	**0.4099**	2.5473	2.8482
55	2.4267	**0.5107**	**4.7396**	**4.7748**

Figure 5.5: Steady-State $\tau = 41$ Control Charts with Shift $\mu = 1$, $\sigma_y = 1$

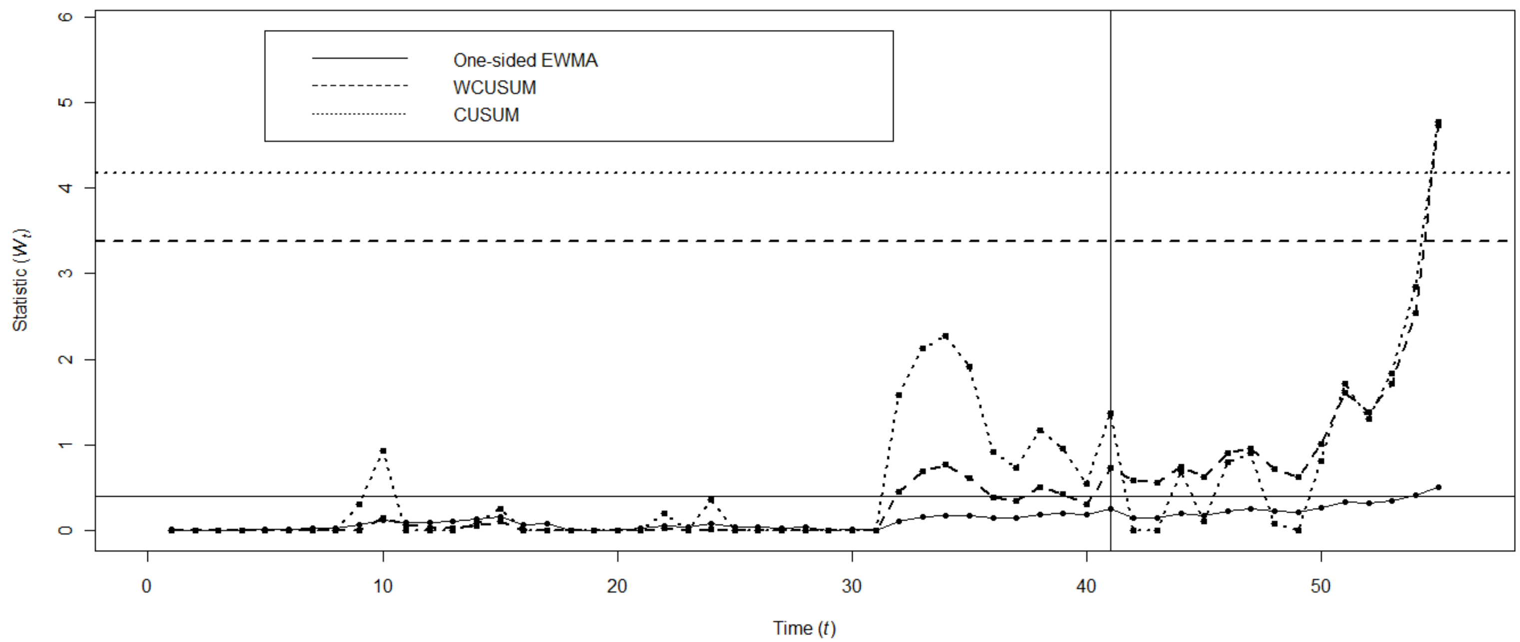

Chapter 6

Conclusions

This thesis proposes the upper-sided EWMA control scheme, which has the feature of adjusting memory magnitudes through the smoothing parameter λ, for monitoring correlated data. The control statistic puts more weight on the more recent observations as the monitoring progresses on. The thesis demonstrates on a variety of time series models that the proposed chart is very efficient for detecting changes in the process mean under the presence of forecast recovery which lead to dynamic patterned mean shifts. The method's performance is enhanced when combined with the fast initial response (FIR) feature which speeds the jump to out-of-control under forecast recovery situations. In practice, a dynamic patterned mean shift has either upper-sided or lower-sided direction, which can be monitored employing either the upper-sided or lower-sided version of the proposed one-sided EWMA control chart. Furthermore, the one-sided EWMA is much more efficient than the two-sided EWMA for detecting one-direction dynamic patterned mean shifts.

The CUSUM control schemes are widely used for monitoring processes due to their simplicity and good performance in standard process monitoring. However, they do not perform well under dynamic mean shifts. Shu, Jiang and Tsui (2008) modified the conventional CUSUM by putting a weight function resulting in the weighted CUSUM (WCUSUM). The basic idea is to enhance the standard CUSUM by putting more weight on observations with higher mean thus trying to push the statistic to the out of control state faster when this happens. The WCUSUM indeed exhibits a far superior performance than the conventional CUSUM control scheme and other alternatives for detecting small to moderate shifts. However, the average run length calculations are much more complicated than for the conventional CUSUM due to the weighting function. A bivariate Markov chain is required for calculating the ARL in the WCUSUM, which requires the dimension of the transition probability matrix to be very large to achieve acceptable accuracy. As a result, one has to calculate the ARL using Monte Carlo simulation, an alternative that also involves larger dimension matrix calculations. An improved Monte Carlo simulation is proposed. It is shown in the thesis that the proposed alternative is much more efficient and that it works very well. The core idea of the improved Monte Carlo simulation is to divide a large dimension calculation into several smaller dimension ones that can be carried out much more efficiently in the computer.

Comparing performance of the upper-sided EWMA with the WCUSUM in forecast recovery situations, the WCUSUM does slightly better than the upper-sided EWMA without the FIR feature. However, the upper-sided EWMA with FIR (HS = 75%) feature does significantly better than the WCUSUM. In non-forecast recovery situations, the performances of the upper-sided EWMA without FIR feature and the WCUSUM are very close while the upper-sided EWMA with FIR feature does much better. Thus, the upper-sided EWMA with FIR feature is overall a better control chart than the WCUSUM.

The most widely used performance measure for control schemes is average run length (ARL), which is the measure adopted in this thesis. When the process operates in-control, the ARL_0 is set to be large in order to reduce the Type I error, that is the frequency of signaling an out of control state when in fact the process is operating well. But for detecting an out-of-control case, the ARL (ARL_1) should be small, that is the method has high power to detect an out-of-control excursion quickly. Thus, run length distribution is important, which requires further study.

The result of the statistical control schemes discussed here are based on six useful but simple ARIMA cases. Further research is required for more complicated ARIMA models or other time series. ARIMA models are widely used for modeling and prediction of financial market activity, economic trends, and ecological and demographic patterns. The proposed upper-sided EWMA control scheme has very good potential as a monitoring tool to detect changes in those processes.

Appendix A

Autoregressive Integrated Moving Average Models

Autoregressive integrated moving average (ARIMA) models typically exhibit forecast recovery. An ARIMA model with p AR components, q MA components and d differences ARIMA(p, d, q) is defined as

$$(1-B)^d \phi(B)(x_t - \mu_0) = \theta(B) a_t$$

or

$$x_t - \mu_0 = \frac{\theta(B)}{(1-B)^d \Phi(B)} a_t \tag{A.1}$$

where B is the back-shift operator, $\phi(B)$ and $\theta(B)$ are polynomials of degrees p and q, respectively, and $a_t's$ are independently and identically distributed (IID) white noise with variance σ_a^2. Here μ_0 represents the mean of the process when it is operating on target. Without loss of generality, $\sigma_a^2 = 1$. They are respectively defined as

$$
\begin{aligned}
Bx_t &= x_{t-1}, \\
\phi(B) &= 1 - \phi_1 B - \phi_2 B^2 - \cdots - \phi_p B^p, \\
\theta(B) &= 1 - \theta_1 B - \theta_2 B^2 - \cdots - \theta_q B^q, \\
a_t &\sim N(0, \sigma_a^2), \\
\mu_0 &= E(x_t).
\end{aligned}
$$

See Chatifield (2004) and Shumway and Stoffer (2006) for a detailed discussion on time series models and methods. Following the standard SPC approach, all the parameters are estimated from a historical (hopefully large) database, usually called Phase I data, gathered when the process was operating on-target. This thesis will not discuss how to estimate the ARIMA model parameters and assumes that all the parameters are known.

When the process is invertible, the residuals can be written as

$$
y_t = \frac{(1-B)^d \phi(B)}{\theta(B)}(x_t - \mu_0). \tag{A.2}
$$

If the process is in-control, the process mean is μ_0 indicating that no drift occurs. i.e., $\mu = E(x_t) = \mu_0$, $t = 1, 2, \cdots$. Suppose the process mean shifts from μ_0 to $\mu_0 + \mu$ at time τ, τ is unknown. Then $f_t = E(x_t) - \mu_0$ will be given by

$$
f_t = \begin{cases} 0 & t = 1, 2, \cdots, \tau - 1; \\ \mu & t = \tau, \tau + 1, \cdots \end{cases}
$$

where $\mu \neq 0$. In this situation, the residuals can be presented as

$$\begin{aligned}
y_t &= \frac{(1-B)^d\phi(B)}{\theta(B)}(x_t-\mu_0) \\
&= \frac{(1-B)^d\phi(B)}{\theta(B)}(x_t-\mu_0-f_t+f_t) \\
&= \frac{(1-B)^d\phi(B)}{\theta(B)}(x_t-\mu_0-f_t)+\frac{(1-B)^d\phi(B)}{\theta(B)}f_t \\
&= a_t+\xi_t \qquad (A.3)
\end{aligned}$$

where

$$\xi_t = \frac{(1-B)^d\phi(B)}{\theta(B)}f_t \qquad (A.4)$$

is the shift that takes place in the residuals, and

$$E(y_t) = E(a_t+\xi_t) = E(a_t)+\xi_t = \xi_t. \qquad (A.5)$$

The shift f_t of x_t causes a mean pattern ξ_t in the residual y_t. Consider the situation where time series x_t has a constant shift μ at time τ and ARIMA(p,d,q) model with $p=1, d=0$, and $q=1$. In this case, taking $\phi=\phi_1$, and $\theta=\theta_1$. Then

$$\begin{aligned}
\xi_t &= \frac{1-\phi B}{1-\theta B}f_t \\
&= (1-\phi B)(1-\theta B)^{-1}f_t
\end{aligned}$$

Hence, ξ_t can be written as

$$\begin{aligned}
\xi_t &= (1-\phi B)(1+\theta B+(\theta B)^2+(\theta B)^3+\cdots)f_t \\
&= (1+\theta B+(\theta B)^2+(\theta B)^3+\cdots-\phi\theta-\phi\theta B^2-\phi\theta^2B^3-\cdots)f_t \\
&= (1+(\theta-\phi)B+\theta(\theta-\phi)B^2+\theta^2(\theta-\phi)B^3+\cdots)f_t \\
&= f_t+(\theta-\phi)Bf_t+\theta(\theta-\phi)B^2f_t+\theta^2(\theta-\phi)B^3f_t+\cdots \\
&= f_t+(\theta-\phi)f_{t-1}+\theta(\theta-\phi)f_{t-2}+\theta^2(\theta-\phi)f_{t-3}+\cdots
\end{aligned}$$

The constant shift μ on time series x_t at and after time τ,

$$f_t = \begin{cases} 0 & t = 1, 2, \cdots, \tau - 1; \\ \mu & t = \tau, \tau + 1, \cdots \end{cases}$$

leads to

$$E(y_t) = \xi_t = \begin{cases} 0 & t = 1, 2, \cdots, \tau - 1; \\ \mu & t = \tau. \end{cases}$$

For $t = \tau + k$, where $k = 1, 2, \cdots$

$$\begin{aligned} E(y_{\tau+k}) &= \xi_{\tau+k} \\ &= (1 - \phi B)(1 + \theta B + (\theta B)^2 + (\theta B)^3 + \cdots) f_{\tau+k} \\ &= f_{\tau+k} + (\theta - \phi) f_{\tau+k-1} + \theta(\theta - \phi) f_{\tau+k-2} + \theta^2(\theta - \phi) f_{\tau+k-3} + \cdots + \\ &\quad \theta^{i-1}(\theta - \phi) f_{\tau+k-i} + \cdots \end{aligned}$$

Note that

$$f_{\tau+k-i} = \begin{cases} \mu & i = 0, 1, 2, \cdots, k; \\ 0 & i > k \end{cases}$$

Thus,

$$\begin{aligned} E(y_{\tau+k}) &= \xi_{\tau+k} \\ &= \mu + (\theta - \phi)\mu + \theta(\theta - \phi)\mu + \theta^2(\theta - \phi)\mu + \cdots + \theta^{k-1}(\theta - \phi)\mu \\ &= (1 + (\theta - \phi)(1 + \theta + \theta^2 + \cdots + \theta^{k-1}))\mu \\ &= (1 + (\theta - \phi)\frac{1 - \theta^k}{1 - \theta})\mu \\ &= \frac{1 - \theta + (\theta - \phi)(1 - \theta)^k}{1 - \theta}\mu \\ &= \frac{1 - \phi + (\theta - \phi)\theta^k}{1 - \theta}\mu \end{aligned}$$

In addition,

$$\frac{1-\phi+(\theta-\phi)\theta^0}{1-\theta}\mu = \frac{1-\phi+\theta-\phi}{1-\theta}\mu = \mu$$

Hence,

$$\xi_t = E(y_t) = \begin{cases} 0 & t = 1, 2, \cdots, \tau - 1; \\ \frac{1-\phi+(\theta-\phi)\theta^{t-\tau}}{1-\theta}\mu & t = \tau, \tau+1, \cdots \end{cases}$$

Although the shift f_t on the mean of x_t is a constant, its effect on the mean of the residuals y_t is not. It has a dynamic pattern. The sequence ξ_t varies over time and depends on the shift that occurred at time τ.

Appendix B

Markov Chain Method for Average Run Length Calculation Under a Dynamic Mean

B.1 ARL Calculation for the Two-Sided EWMA

Brook and Evans (1972) were the first to develop a Markov chain approach for calculating run length distributions and average run lengths for the conventional CUSUM chart. The procedure applies only to in-control process operation or sustained changes in the process mean. The key step is approximating a continuous-state Markov chain by a finite-state one. The method was extended to the two-sided EWMA by Lucas and Saccucci (1990) for the same context of in-control process operation or sustained jumps in the process mean. In this thesis, we extend the method to the context of a dynamic process mean.

The two-sided EWMA chart statistic is (see eqn. (3.1))

$$W_t = (1 - \lambda)W_{t-1} + \lambda y_t, \quad t = 1, 2, 3, ... \tag{B.1}$$

with W_0 being the initially set chart value, typically $W_0 = 0$. Here λ $(0 \leq \lambda \leq 1)$ is amount of **smoothing**. The chart is usually standardized so that when the process operates on-target, W_t drifts around 0. Further, for the normal case considered here, W_t has a normal distribution centered at 0 under on-target process operation. Accordingly, the typical control limits are set at $\pm h$ where $h > 0$ is selected to achieve a desired on-target average run length ARL_0, in our case $ARL_0 = 400$.

It is easy to see from eqn. (B.1) that W_t forms a continuous-state Markov chain with state space $(-\infty, \infty)$. To construct the finite-state approximating Markov chain, for a given positive integer m we divide the continuous state space into $2m+3$ subintervals which define the chain states. Two states are absorbent, namely

$$E_0 = (-\infty, -h) \quad \text{and} \quad E_{2m+2} = (h, \infty).$$

The remaining states, which are the ones of primary interest, are transient states and come from dividing the in-control range $[-h, h]$ into $2m+1$ equal-width subintervals, $E_1, E_2, ..., E_{2m+1}$, where

$$E_1 = [S_1 - L, S_1 + L], ; \quad E_i = (S_i - L, S_i + L], \; i = 2, 3, ..., 2m + 1,$$

where $S_i = -h + (2i-1)L$ is the center of state E_i and $L = h/(2m+1)$. We say that the chain is in state E_i at sampling period t if $W_t \in E_i$.

The probabilities with which the statistic moves among the transient states as we go from sampling period $t-1$ to t are collected in the associated $(2m+1)\times(2m+1)$

transition probability matrix, denoted by $\boldsymbol{P}_t$ here,

$$\boldsymbol{P}_t = \begin{pmatrix} P_{11}^{(t)} & P_{12}^{(t)} & \dots & P_{1j}^{(t)} & \dots & P_{1,2m+1}^{(t)} \\ P_{21}^{(t)} & P_{22}^{(t)} & \dots & P_{2j}^{(t)} & \dots & P_{2,2m+1}^{(t)} \\ \vdots & \vdots & \vdots & \vdots & \vdots & \vdots \\ P_{i1}^{(t)} & P_{i2}^{(t)} & \dots & P_{ij}^{(t)} & \dots & P_{i,2m+1}^{(t)} \\ \vdots & \vdots & \vdots & \vdots & \vdots & \vdots \\ P_{2m+1,1}^{(t)} & P_{2m+1,2}^{(t)} & \dots & P_{2m+1,j}^{(t)} & \dots & P_{2m+1,2m+1}^{(t)} \end{pmatrix}.$$

The transition probability from state i to state j is

$$\begin{aligned} P_{ij}^{(t)} &= Pr\{W_t \in E_j \mid W_{t-1} \in E_i\} \\ &= Pr\{S_j - L < W_t \le S_j + L \mid S_i - L < W_{t-1} \le S_i + L\} \\ &\approx Pr\{S_j - L < (1-\lambda)W_{t-1} + \lambda y_t \le S_j + L \mid W_{t-1} = S_i\} \\ &= Pr\left\{\frac{L}{\lambda}[2(j-(1-\lambda)i)-1] - h - L < y_t < \frac{L}{\lambda}[2(j-(1-\lambda)i)+1] - h - L\right\}. \end{aligned}$$

Under a dynamic mean, assume the process mean at sampling period t is μ_t. The process variance may stay in control or not, consider the general case of a changing process variance σ_t^2. We assume a normal distribution under independent observations, thus $y_1, y_2, ...$ are independent with $y_t \sim N(\mu_t, \sigma_t^2)$. It follows then that

$$\begin{aligned} P_{ij}^{(t)} \approx \Phi &\left(\frac{1}{\sigma_t}\left\{\frac{L}{\lambda}[2(j-(1-\lambda)i)+1] - h - L - \mu_t\right\}\right) \\ -\Phi &\left(\frac{1}{\sigma_t}\left\{\frac{L}{\lambda}[2(j-(1-\lambda)i)-1] - h - L - \mu_t\right\}\right) \end{aligned} \tag{B.2}$$

Note that this approximation improves as m increases. In the work done in this thesis, m around 50 gives satisfactory results. In the rest of Appendix B we will replace the "approximate" sign with the "equal" sign.

The first interesting feature to notice here is that the transition probabilities vary over t resulting in a **non-homogeneous Markov chain**. The **run length** RL is the number of sampling periods observed until and including the sampling period when the statistic jumps to an absorbing state for the first time. Clearly $RL \in \{1, 2, ...\}$. From the theory of Markov chains (e.g. see Karlin and Taylor (1975, Chaps. 2-3)) we know that

$$\begin{aligned} Pr(RL > n) &= \boldsymbol{p}_0' \boldsymbol{P}_1 \boldsymbol{P}_2 \cdots \boldsymbol{P}_n \mathbf{1} \\ &= \boldsymbol{p}_0' \left(\prod_{l=1}^{n} \boldsymbol{P}_l \right) \mathbf{1}, \quad n = 1, 2, 3, ..., \end{aligned} \tag{B.3}$$

where $\boldsymbol{p}_0$ is the $(2m+1) \times 1$ initial probability vector on the transient states and $\mathbf{1}$ is the $(2m+1) \times 1$ vector of 1s.

Hence the probability mass function (pmf) of the run length is

$$\begin{aligned} f_{RL}(n) &= Pr(RL = n) \\ &= Pr(RL > n-1) - Pr(RL > n) \\ &= \boldsymbol{p}_0' \left(\prod_{l=1}^{n-1} \boldsymbol{P}_l \right) (\boldsymbol{I} - \boldsymbol{P}_n)\mathbf{1}, \quad n = 1, 2, 3, ... \end{aligned} \tag{B.4}$$

The resulting **average run length** is therefore

$$\begin{aligned} ARL = E(RL) &= \sum_{n=1}^{\infty} n f_{RL}(n) \\ &= \sum_{n=1}^{\infty} n \boldsymbol{p}_0' \left(\prod_{l=1}^{n-1} \boldsymbol{P}_l \right) (\boldsymbol{I} - \boldsymbol{P}_n)\mathbf{1} \end{aligned} \tag{B.5}$$

A special case of particular interest is that where the means and variances are the same across t, that is, $\mu_t = \mu$ and $\sigma_t^2 = \sigma^2$ for all t. This leads to an **homogeneous Markov Chain**. Replacing $\boldsymbol{P}_t = \boldsymbol{P}$, for all t in (B.4) yields run length pmf

$$f_{RL}(n) = \boldsymbol{p}_0' \boldsymbol{P}^{n-1}(\boldsymbol{I} - \boldsymbol{P})\mathbf{1}, \quad n = 1, 2, 3, ... \tag{B.6}$$

And the resulting average run length from (B.5) becomes

$$\begin{aligned} ARL = \sum_{n=1}^{\infty} n\boldsymbol{p}_0' \boldsymbol{P}^{n-1}(\boldsymbol{I} - \boldsymbol{P})\mathbf{1} &= \boldsymbol{p}_0' \left(\sum_{n=1}^{\infty} n\boldsymbol{P}^{n-1} \right) (\boldsymbol{I} - \boldsymbol{P})\mathbf{1} \\ &= \boldsymbol{p}_0' (\boldsymbol{I} - \boldsymbol{P})^{-1}\mathbf{1}. \end{aligned} \tag{B.7}$$

Equations (B.6)-(B.7) were derived by Lucas and Saccucci (1990) in their analysis of the two-sided EWMA for in-control process operations or step mean changes. In particular, Lucas and Saccucci (1990) make extensive use of eqn. (B.7) to calculate the ARL when the process operates on-target or when the process jumps to another mean value from the very beginning (the so called zero-state).

B.2 ARL Calculation for the Upper-Sided EWMA

The upper-sided EWMA of interest here is the upper-sided version given by eqn. (3.2), namely

$$W_t^+ = \max\{0, (1 - \lambda)W_{t-1}^+ + \lambda y_t\}, \quad t = 1, 2, 3, ... \tag{B.8}$$

where the smoothing parameter λ and y_t are as in the two-sided EWMA just discussed, and $W_0^+ = 0$. Clearly $W_t^+ \in [0, \infty)$ with large values indicative of possible departure from on-target process operation in the direction of a larger mean. Thus, only an upper control limit $h > 0$ is needed. Again, one can readily show that W_t^+ forms a continuous-state Markov chain with $[0, \infty)$ as its state space.

The finite-state approximating chain will be constructed as follows. For every integer $m > 0$ there will be m transient states and an absorbent state. The absorbent state will be $E_{m+1} = (h, \infty)$ while the transient states $E_1, E_2, ..., E_m$ will be obtained by dividing the decision interval $[0, h]$ into m subintervals of which the first has length L and the remaining ones length $2L$ where $L = h/(2m-1)$. Specifically, $E_1 = [S_1, S_1 + L]$ and $E_i = (S_i - L, S_i + L]$ where $S_i = 2(i-1)L$, $i = 1, 2, ..., m$. At any sampling period t, the control statistic W_t^+ is said to be in state E_i if $W_t^+ \in E_i$. Again, for the purpose of run length distribution and average run length calculations, we need to consider only the transient states.

The probabilities with which the control statistic moves among the transient states as we go from sampling period $t-1$ to t are collected in the associated $m \times m$ transition probability matrix which we denote by $\boldsymbol{P}_t$,

$$\boldsymbol{P}_t = \begin{pmatrix} P_{11}^{(t)} & P_{12}^{(t)} & \dots & P_{1j}^{(t)} & \dots & P_{1m}^{(t)} \\ P_{21}^{(t)} & P_{22}^{(t)} & \dots & P_{2j}^{(t)} & \dots & P_{2m}^{(t)} \\ \vdots & \vdots & \vdots & \vdots & \vdots & \vdots \\ P_{i1}^{(t)} & P_{i2}^{(t)} & \dots & P_{ij}^{(t)} & \dots & P_{im}^{(t)} \\ \vdots & \vdots & \vdots & \vdots & \vdots & \vdots \\ P_{m1}^{(t)} & P_{m2}^{(t)} & \dots & P_{mj}^{(t)} & \dots & P_{mm}^{(t)} \end{pmatrix}.$$

For $i \geq 2$ and $j \geq 2$, the transition probability from state i to state j can be written as

$$
\begin{aligned}
P_{ij}^{(t)} &= Pr\{W_t^+ \in E_j \ \mid \ W_{t-1} \in E_i\} \\
&= Pr\{S_j - L < W_t^+ \leq S_j + L \ \mid \ S_i - L < W_{t-1}^+ \leq S_i + L\} \\
&= Pr\{S_j - L < \max\{0, (1-\lambda)W_{t-1}^+ + \lambda y_t\} \leq S_j + L \ \mid \ S_i - L < W_{t-1}^+ \leq S_i + L\} \\
&= Pr\{S_j - L < (1-\lambda)W_{t-1}^+ + \lambda y_t \leq S_j + L \ \mid \ S_i - L < W_{t-1}^+ \leq S_i + L\} \\
&\approx Pr\{S_j - L < (1-\lambda)W_{t-1}^+ + \lambda y_t \leq S_j + L \ \mid \ W_{t-1}^+ = S_i\} \\
&= Pr\left\{\frac{L}{\lambda}[2(j-(1-\lambda)(i-1)) - 3] < y_t \leq \frac{L}{\lambda}[2(j-(1-\lambda)(i-1)) - 1]\right\}.
\end{aligned}
$$

If the residual y_t is normally distributed with a dynamic mean μ_t over time and a possibly time-varying variance σ_t^2, that is $y_t \sim N(\mu_t, \sigma_t^2)$, then the transition probability $P_{ij}^{(t)}$ is

$$
\begin{aligned}
P_{ij}^{(t)} \approx \Phi&\left(\frac{1}{\sigma_t}\left\{\frac{L}{\lambda}[2(j-(1-\lambda)(i-1)) - 1] - \mu_t\right\}\right) \\
-\Phi&\left(\frac{1}{\sigma_t}\left\{\frac{L}{\lambda}[2(j-(1-\lambda)(i-1)) - 3] - \mu_t\right\}\right). \qquad \text{(B.9)}
\end{aligned}
$$

Eqn. (B.9) also applies to $i = 1$. Consider now $j = 1$ and $i \geq 2$. Following the same reasoning, the respective transition probability can be approximated through the following equation

$$
P_{i1}^{(t)} \approx \Phi\left(\frac{1}{\sigma_t}\left\{\frac{L}{\lambda}[1 - 2(1-\lambda)(i-1)] - \mu_t\right\}\right). \qquad \text{(B.10)}
$$

The formula is also valid for $i = 1$.

Note that, as was the case for the two-sided EWMA, under a time-changing mean and variance for y_t, the transition probability matrix $\boldsymbol{P}_t$ changes with t. Thus the finite-state approximating Markov chain is non-homogeneous. Equations (B.3)-

(B.5) apply using the $m \times m$ transition probability matrix $\boldsymbol{P}_t$ just calculated. Moreover, when μ_t and σ_t^2 are fixed, equal to μ and σ^2 say, for all t, the chain is homogeneous. Writing $\boldsymbol{P}_t = \boldsymbol{P}$ for all t, equations (B.6)-(B.7) can be used to obtain the respective run length pmf and average run length.

B.3 ARL Calculation for the One-Sided CUSUM

The upper-sided CUSUM enjoys greater attention than the upper-sided EWMA. We consider the upper-version of it for the same reasons we focused on the upper-sided EWMA. The chart statistic is given by

$$S_t^+ = \max\{0, S_{t-1}^+ + y_t - k\}, \quad t = 1, 2, 3, ... \tag{B.11}$$

where k is the **reference value**. While the optimal k is given by $k = (\mu_0 + \mu_1)/2$ when we aim to detect a sustained change in process mean from $\mu = \mu_0$ to $\mu = \mu_1 > \mu_0$, however when we deal with a dynamic mean there is no optimal value and one ends up trying out several values.

Again from eqn. (B.11) one can readily verify that S_t^+ forms a Markov chain. The approach to calculate run length distribution and average run length follows the same steps as for the upper-sided EWMA. In particular, the state space is the same. The only and important difference is the way the $m \times m$ transition probability matrix $\boldsymbol{P}_t$ is calculated. For $i \geq 1$ and $j \geq 2$, the transition probability of moving from state i at sampling period $t-1$ to state j at t is

$$\begin{aligned} P_{ij}^{(t)} &\approx Pr\{[2(j-i)-1]L + k < y_t \leq [2(j-i)+1]L + k\} \\ &= \Phi\left(\frac{1}{\sigma_t}\{[2(j-i)+1]L + k - \mu_t\}\right) - \Phi\left(\frac{1}{\sigma_t}\{[2(j-i)-1]L + k - \mu_t\}\right), \end{aligned} \tag{B.12}$$

where the errors $y_1, y_2, y_3, ...$ are independent with $y_t \sim N(\mu_t, \sigma_t^2)$. The respective $P_{i1}^{(t)}$ transition probability is

$$P_{i1}^{(t)} \approx Pr\{S_{t-1}^{+} + y_t - k \leq L \;\mid\; S_{t-1}^{+} = 2(i-1)L)\}$$

$$= \Phi\left(\frac{1}{\sigma_t}\{k - (2i-3)L - \mu_t\}\right). \tag{B.13}$$

Again, under a time-varying mean and variance for y_t, the transition probability matrix $\boldsymbol{P}_t$ changes with t resulting in a non-homogeneous finite-state approximating chain. Equations (B.3)-(B.5) can be used to calculate run length pmf's and average run lengths where $\boldsymbol{P}_t$ is the $m \times m$ transition probability matrix with entries given by (B.12)-(B.13). Moreover, when μ_t and σ_t^2 are fixed, equal to μ and σ^2 say, for all t, the chain is homogeneous. Writing $\boldsymbol{P}_t = \boldsymbol{P}$ for all t, equations (B.6)-(B.7) can be used to obtain the respective run length pmf and average run length. These latter formulas were originally developed by Brooks and Evans (1972). They are useful to calculate on-target average run lengths.

Appendix C

Monte Carlo Simulation Algorithm of ARIMA Models for the WCUSUM Control Scheme

Monte Carlo simulation is a computational algorithm that relies on repeated random sampling to compute its results. Here, there are six ARIMA$(1, 0, 1)$ time series models as detailed in Table 1.1. Monte Carlo simulation of the WCUSUM control scheme under ARIMA$(1, 0, 1)$ data can be constructed by the following procedures:

Step 1**.** Find the distribution of the random variable.

From Equation (A.3)

$$y_t = a_t + \xi_t$$

where $a_t \sim N(0,1)$ and

$$\xi_t = E(y_t) = \begin{cases} 0 & t = 1, 2, \cdots, \tau - 1; \\ \frac{1-\phi+(\theta-\phi)\theta^{t-\tau}}{1-\theta}\mu & t = \tau, \tau+1, \cdots \end{cases}$$

It is easy to see that $y_t \sim N(\xi_t, 1)$.

Step 2. Find the relationship between the weight Q_t and random variable y_t.

From Equation (2.5)

$$\begin{aligned} Q_t &= (1-\lambda)Q_{t-1} + \lambda y_t \\ &= (1-\lambda)((1-\lambda)Q_{t-2} + \lambda y_{t-1}) + \lambda y_t \\ &= (1-\lambda)^t Q_0 + \lambda((1-\lambda)^{t-1} y_1 + (1-\lambda)^{t-2} y_2 + \cdots + (1-\lambda) y_{t-1} + y_t) \end{aligned}$$

Usually, $Q_0 = 0$,

$$Q_t = \lambda((1-\lambda)^{t-1} y_1 + (1-\lambda)^{t-2} y_2 + \cdots + (1-\lambda) y_{t-1} + y_t). \tag{C.1}$$

Step 3. Randomly generate n independent values of y_t based on normal distribution $N(\xi_t, 1)$, $t = 1, 2, \cdots, n$.

The number n can be considered as the maximum run length. It is suggested that n be chosen as large or equal to ten times the desired average run length. For instance, $n = 4000$ if $ARL = 400$.

Step 4. Construct a n dimension vector $\boldsymbol{Q}$

$$\boldsymbol{Q} = \begin{pmatrix} \lambda y_1 \\ \lambda(1-\lambda)y_1 + \lambda y_2 \\ \cdot \\ \cdot \\ \cdot \\ \lambda((1-\lambda)^{n-1} y_1 + (1-\lambda)^{n-2} y_2 + \cdots + (1-\lambda) y_{n-1} + y_n) \end{pmatrix}$$

Let $\boldsymbol{\lambda} = (\lambda, \lambda(1-\lambda), \cdots, \lambda(1-\lambda)^{n-1})'$, and

$$\boldsymbol{Y}_{n\times n} = \begin{pmatrix} y_1 & 0 & 0 & \cdots & 0 & 0 \\ y_2 & y_1 & 0 & \cdots & 0 & 0 \\ \cdot & \cdot & \cdot & \cdots & 0 & 0 \\ \cdot & \cdot & \cdot & \cdots & 0 & 0 \\ \cdot & \cdot & \cdot & \cdots & y_1 & 0 \\ y_n & y_{n-1} & y_{n-2} & \cdots & y_2 & y_1 \end{pmatrix}$$

then

$$\boldsymbol{Q} = \boldsymbol{Y}_{n\times n}\boldsymbol{\lambda} \tag{C.2}$$

Step 5. Calculate run length.

From Equation (2.4),

$$W_t = \max\{0, W_{t-1} + (y_t - k)|Q_t|\}.$$

The process starts from $W_0 = 0$, n values of $y_t's$ are generated at Step 3, and n values of $Q_t's$ are calculated at Step 4, W_t is iteratively calculated based on the above equation. When $W_t \geq h$, the run length (RL) is the number of t, i.e. $RL = t$.

Step 6. Calculate average run length.

Repeat the above N times to get run length values $RL_1, RL_2, \cdots, RL_N$. The Simulated average run length (ARL) is the average of N run length values,

$$ARL = \frac{\sum_{i=1}^{N} RL_i}{N}. \tag{C.3}$$

Usually $N = 160,000$.

Bibliography

[1] Abbasi A. S. (2010). On Sensitivity of EWMA Control Chart for Monitoring Process Dispersion. *Proceedings of the World Congress on Engineering*, **3**, 2027-2032.

[2] Alwan, L. C. and Roberts, H. V. (1988). Time Series Modeling for Statistical Process Control. *Journal of Business & Economic Statistics*, **6**, 87-95.

[3] Apley, D. W. and Shi, J. (1999). The GLRT for Statistical Process Control of Autocorrelated Process. *IIE Transactions*, **31**, 1123-1134.

[4] Barr, D. R. and Sherrill, T. E. (1999). Mean and Variance of Truncated Normal Distributions. *The American Statistician*, **53**, 357-361.

[5] Brook, D. and Evans, D. A. (1972). An Approach to the Probability Distribution of CUSUM Run Length. *Biometrika*, **40**, 539-549.

[6] Chang, C. T. and Gan, F. F. (1994). Optimal Designs of One-sided EWMA Charts for Monitoring a Process Variance. *Journal of Statistical Computation and Simulation*, **49**, 33-48.

[7] Chatfield C. (2004). *The Analysis of Time Series An Introduction*, Chapman & Hall/CRC.

[8] Crowder, S. V. (1987). A Simple Method for Studying Run Length Distributions of Exponentially Weighted Moving Average Control Charts. *Technometrics*, **29**, 402-407.

[9] Gan, F. F. (1998). Designs of One-sided and Two-sided Exponential EWMA Charts. *Journal of Quality Technology*, **30**, 55-69.

[10] Hawkins, M. D. and Olwell, H. D. (1998). *Cumulative Sum Charts and Charting for Quality Improvement*, New York: Springer-Verlag.

[11] Hu, S. J. and Roan, C. (1996). Change patterns of time series-based control charts. *Journal of Quality Technology*, **28**, 302-312.

[12] Hunter, J. S. (1986). The Exponentially Weighted Moving Average. *Journal of Quality Technology*, **18**, 203-210.

[13] Huwang, L., Huang, C. and Wang, Y. (2010). New EWMA Control Charts for Monitoring Process Dispersion. *Computation Statistics and Data Analysis*, **54**, 2328-2342.

[14] Jiang, W., Shu, L. and Apley, W. D. (2008). Adaptive CUSUM procedures with EWMA-based shift estimators. *IIE Transactions*, **40**, 992-1103.

[15] Karlin, S. and Taylor, H. M. (1975). *A First Course in Stochastic Processes*, Second Edition, New York: Academic Press.

[16] Knoth, S. (2005). Fast Initial Response Features for EWMA Control Charts. *Statistics Papers*, **46**, 47-64.

[17] Li, Z. and Wang, Z. (2010). Research Article Adaptive CUSUM of Q chart. *International Journal of Production Research*, **48**, 1287-1301.

[18] Lucas, J. M. and Crosier, R. B. (1982). Fast Initial Response for CUSUM Quality-Control Schemes: Give Your CUSUM a Head Start. *Technometrics*, **24**, 199-205.

[19] Lucas, J. M. and Saccucci, M. S. (1990). Exponentially Weighted Moving Average Control Schemes: Properties and Enhancements. *Technometrics*, **32**, 1-29.

[20] Luceño, A. (1999). Average run lengths and run length probability distributions for cuscore charts to control normal mean. *Journal Computational Statistics & Data Analysis*, **32**, 177-195.

[21] Luceño, A. and Puig-pey, J. (2000). Evaluation of the Run Length Probability Distribution for CUSUM Charts: Assessing Chart Performance. *Technometrics*, **42**, 411-416.

[22] Montgomery, C. D. (2005). *Introduction to Statistical Quality Control Fifth Edition*, John Wiley & Sons, Inc.

[23] Moustakes, G.V. (1986). Optimal Stopping Times for Detecting Changes in Distributions. *The Annals of Statistics*, **14**, 1379-1387.

[24] Roberts, S. W. (1959). Control Chart Tests based on Geometric Moving Average. *Technometrics*, **1**, 239-250.

[25] Robinson, P. B. and Ho, T. Y. (1978). Average Run Lengths of Geometric Moving Average Charts by Numerical Methods. *Technometrics*, **20**, 85-93.

[26] Shu, L. and Jiang, W. (2006). A Markov Chain Model for the Adaptive CUSUM Control Chart. *Journal of Quality Technology*, **38**, 135-147.

[27] Shu, L., Jiang, W. and Tsui, K. (2008). A Weighted CUSUM Chart for Detecting Patterned Mean Shifts. *Journal of Quality Technology*, **40**, 194-213.

[28] Shu, L., Jiang, W. and Wu, S. (2007). A One-sided EWMA Control Chart for Monitoring Process Means. *Communication in Statistics - Simulation and Computation*, **36**, 901-920.

[29] Shu, L., Jiang, W. and Wu, Z. (2008). Adaptive CUSUM Procedures with Markovian Mean Estimation. *Computational Statistics & Data Analysis*, **52**, 4395-4409.

[30] Shumway, R. H. and Stoffer, D. S. (2006). *Time Series Analysis and its Application with R Examples*, New York: Springer Science.

[31] Steiner, H. S. (1999). EWMA Control Charts with Time-Varying Control Limits and Fast Initial Response. *Journal of Quality Technology*, **31**, 75-86.

[32] Waldmann, K. H. (1986). Bounds for the Distribution of the Run Length of the Geometric Moving Average Charts. *Applied Statistics*, **35**, 151-158.